ELSEVIER

Journal of Hepatology 46 (2007) 26–36

Journal of Hepatology

www.elsevier.com/locate/jhep

Serum-derived hepatitis C virus infectivity in interferon regulatory factor-7-suppressed human primary hepatocytes

Hussein H. Aly[1,2,3], Koichi Watashi[2], Makoto Hijikata[2], Hiroyasu Kaneko[2], Yasutugu Takada[1], Hiroto Egawa[1], Shinji Uemoto[1], Kunitada Shimotohno[2,*]

[1]*Graduate School of Medicine, Department of Transplant Surgery, Kyoto University Hospital, Kyoto, Japan*
[2]*Laboratory of Human Tumor Viruses, Institute of Virus Research, Kyoto University, Japan*
[3]*Hepatology Department, National Hepatology and Tropical Medicine Research Institute, Cairo, Egypt*

See Editorial, pages 1–5

Background/Aims: **The development of an efficient in vitro infection system for HCV is important in order to develop new anti-HCV strategy. Only Huh7 hepatocyte cell lines were shown to be infected with JFH-1 fulminant HCV-2a strain and its chimeras. Here we aimed to establish a primary hepatocyte cell line that could be infected by HCV particles from patients' sera.**

Methods: **We transduced primary human hepatocytes with human telomerase reverse transcriptase together with human papilloma virus 18/E6E7 (HPV18/E6E7) genes or simian virus large T gene (SV40 T) to immortalize cells. We also established the HPV18/E6E7-immortalized hepatocytes in which interferon regulatory factor-7 was inactivated. Finally we analyzed HCV infectivity in these cells.**

Results: **Even after prolonged culture HPV18/E6E7-immortalized hepatocytes exhibited hepatocyte functions and marker expression and were more prone to HCV infection than SV40 T-immortalized hepatocytes. The susceptibility of HPV18/E6E7-immortalized hepatocytes to HCV infection was further improved, in particular, by impairing signaling through interferon regulatory factor-7.**

Conclusions: **HPV18/E6E7-immortalized hepatocytes are useful for the analysis of HCV infection, anti-HCV innate immune response, and screening of antiviral agents with a variety of HCV strains.**

Keywords: **Immortalization; Primary hepatocytes; HCV infection; IRF-7; IRF-3; HPV18/E6E7; Innate immune response**

1. Introduction

Infection with Hepatitis C virus (HCV) is a serious problem worldwide since 3% of the world's population is chronically infected [1]. Chronic HCV may lead to liver cirrhosis and hepatocellular carcinoma. Current standard therapy utilizes the combination of pegylated interferon-α and ribavirin, which results in a sustained response in only 30–60% of patients [2–5]. Many patients, however, do not qualify for or tolerate standard therapy [6]. Thus, it is important to develop an efficient in vitro infection system for HCV to facilitate the discovery of new anti-HCV strategies. Only Huh7 cell line is permissive for replication, infection and release of the fulminant hepatitis-derived HCV-2a (JFH-1) *strain* and its chimeric derivatives [7–9]. No other hepatocyte cell lines are able to support HCV replication efficiently.

Received 5 June 2006; received in revised form 24 July 2006; accepted 1 August 2006; available online 30 October 2006

* Corresponding author. Tel.: +81 75 751 4000; fax: +81 75 751 3998.
E-mail address: kshimoto@virus.kyoto-u.ac.jp (K. Shimotohno).

0168-8278/$32.00
doi:10.1016/j.jhep.2006.08.018

Normal human hepatocytes are the ideal system in which to study HCV infectivity. When cultured in vitro, however, they proliferate poorly and divide only a few times [10]. Continuous proliferation could be achieved however by introducing oncogenes, such as Simian virus large tumor antigen (SV40 T) [11]. This often resulted in tumor development [12] together with numerical (aneuploidy) and structural (aberrations) chromosome abnormalities [13]. The human papilloma virus E6E7 genes (HPV/E6E7) immortalized multiple cell types that were phenotypically and functionally similar to the parental cells [14–20]. As yet, no human hepatocytes have been immortalized with HPV18/E6E7.

We established a human primary non-neoplastic hepatocyte cell line transduced with the HPV18/E6E7 that retained primary hepatocyte characteristics even after prolonged culture, and were more prone to HCV infection than those cells immortalized with SV40 T antigen. We further improved the susceptibility of HPV18/E6E7-immortalized hepatocytes to HCV infectivity by impairing interferon regulatory factor-7 (IRF-7) expression. These cells are useful to assay infectivity of HCV strains other than JFH-1, HCV replication, innate immune system engagement of HCV, and screening of anti-HCV agents. This infection system using non-neoplastic cells also suggested that IRF-7 plays an important role in eliminating HCV infection.

2. Materials and methods

2.1. Cell cultures

We obtained the approval of the Ethical Committee of Kyoto University for the use of human hepatocytes and sera obtained from HCV-positive patients. Informed consent was obtained from both the hepatocyte donor and HCV-positive patients. Primary hepatocytes (P.H.) were cultured as described [21]. HeLa, 293, Huh-7.5, and PH5CH8 cells were cultured as previously described [22]. For three-dimensional (3D) cultures, Mebiol Gel (Mebiol Inc.) was prepared according to the manufacturer's instructions.

2.2. Plasmids construction

The SV40 T, hTERT and HPV/E6E7 fragments from pAct-SVT, PCX4neo/hTERT, and pLXSN-E6E7 plasmids were inserted into pCSII-EF-RFA plasmid creating the pCSII-EF-SVT, pCSII-EF-hTERT, and pCSII-EF-E6E7 plasmids, respectively. The full-length IRF-3 and IRF-7 genes were cloned by RT-PCR using total RNA isolated from 293 cells as a template and were inserted into pcDNA3 vector. Dominant-negative forms of IRF-3 (DNIRF-3) and IRF-7 (DNIRF-7) were constructed by PCR amplification of the coding region for amino acid residues 108–427 of IRF-3 and 237-514 of IRF-7, respectively. The amplified IRF-3 fragment was cloned into pcDNA3 in frame with a FLAG epitope tag generating pcFLAG-DNIRF-3. The amplified IRF-7 fragment was cloned into pLXSH in frame with HA epitope tag generating pLXSH-HA-DNIRF-7. The pIFNβ promoter-luc and pIFNα promoter-luc plasmids were gifts from Dr. Taniguchi of the Tokyo University. The psiRNA-hIRF-3 and psiRNA-hIRF-7 plasmids were purchased from Invivogen (USA).

2.3. Immunoblot analysis

Immunoblot analysis was performed as described previously [22]. We used anti-SV40 T (Santa Cruz), anti-HPV18/E7 (Santa Cruz), anti-tubulin (Sigma), anti-FLAG (Sigma), and anti-HA (Sigma) antibodies.

2.4. Transfection, small interfering RNA silencing and luciferase assays

Transfection of plasmid DNA was performed using Effectene transfection reagent (Qiagen) as recommended by the manufacturer. The pLXSH-HA-DNIRF-7 plasmid was transfected into the HuS-E/2 clone; transfectants were selected in 100 μg/ml hygromycin B (Gibco). The psiRNA-hIRF-3 and psiRNA-hIRF-7 plasmids were separately transfected into HuS-E/2 cells followed by Zeocin (250 μg/ml) selection. After two weeks of continuous selection, cells were infected with HCV. Luciferase assays were conducted as previously described [22]. The results are presented as relative light units (RLU) normalized to the total content of protein in the cell lysates.

2.5. Reverse transcriptase polymerase chain reaction (RT-PCR) and real-time RT-PCR

Using 250 ng of total RNA as a template, we performed RT-PCR with a one-step RNA PCR kit (Takara) according to the manufacturer's instructions. The primer sets and reaction conditions used are detailed in Table 1. To measure HCV-RNA titers by real-time RT-PCR, we collected RNA from infected wells. Five hundred nanograms of total cellular RNA was analyzed for the quantity of HCV-RNA as previously described [23].

2.6. HCV infection experiment

HCV infection experiment from serum was done as mentioned before [22]. HCV-infected-serums were titrated and 1×10^5 HCV-RNA copies/ml were used for each infection experiment. Concentrated culture medium for HCV/JFH1-producing cells was prepared as previously described [7]. HCV titer in the concentrated medium was measured, adjusted and added to the cells as mentioned above.

2.7. Blocking of HCV infectivity by anti-CD81

Inhibition of HCV infectivity was performed by blocking CD81 as previously described [7].

3. Results

3.1. Establishment of immortalized primary human hepatocytes

Primary hepatocytes were isolated from liver tissue obtained from a 9-year-old male patient with Primary Hyperoxaluria who had undergone liver transplantation. Hepatocytes were left unmanipulated or transduced with CSII-EF-hTERT alone or in combination with CSII-EF-SVT or CSII-EF-E6E7 to enhance the efficiency of immortalization. After six weeks only cells transduced by the combination of hTERT and either LT or HPV18/E6E7 continued to proliferate. Initially appearing colonies with a growth advantage were picked up and expanded. SV40 T-immortalized cell clones were named HuS-T cells and given numbers from 1 to 7,

Table 1
Primer sequences and RT-PCR parameters

Genes	Primer sequence 5′–3′	PCR parameters[a]
HGF	F: AGGAGCCAGCCTGAATGATGA R: CCCTCTGATGTCCCAAGATTAGC	95, 56, 72 1 min, 45 s, 1 min
TGFα	F: ATGGTCCCCTCGGCTGGA R: GGCCTGCTTCTTCTGGCTGGCA	95, 59, 72 45 s, 30 s, 1 min
TGFβ1	F: GCCCTGGACACCAACTATTGCT R: AGGCTCCAAATGTAGGGGCAGG	95, 58, 72 45 s, 30 s, 1 min
TGFβ2	F: GATTTCCATCTACAAGACCACGAGGGACTTGC R: CAGCATCAGTTACATCGAAGGAGAGCCATTCG	95, 58, 72 45 s, 30 s, 1 min
HGFR	F: TGGTCCTTGGCGTCGTCCTC R: CTCATCATCAGCGTTATCTTC	95, 54, 72 30 s, 45 s, 1 min
EGFR	F: CTACCACCACTCTTTGAACTGGACCAAGG R: TCTATGCTCTCACCCCGTTCCAAGTATCG	95, 58, 72 45 s, 30 s, 1 min
TGFβ1R	F: CGTGCTGACATCTATGCAAT R: AGCTGCTCCATTGGCATAC	95 s, 54, 72 30 s, 45 s, 1 min
TGFβ2R	F: TGCACATCGTCCTGTGGAC R: GTCTCAAACTGCTCTGAAGTGTTC	95, 58, 72 45 s, 30 s, 1 min
FGFR	F: ATGTGGAGCTGGAAGTGCCTC R: GGTGTTATCTGTTTCTTTCTCC	95, 54, 72 30 s, 45 s, 1 min
IGF-1R	F: ACCCGGAGTACTTCAGCGCT R: CACAGAAGCTTCGTTGAGAA	95, 54, 72 30 s, 45 s, 1 min
HNF1α	F: GTGTCTACAACTGGTTTGCC R: TGTAGACACTGTCACTAAGG	95, 52, 72 45 s, 30 s, 1 min
HNF1β	F: GAAACAATGAGATCACTTCCTCC R: CTTTGTGCAATTGCCATGACTCC	95, 52, 72 1 m, 45 s, 1 min
HNF3β	F: CACCCTACGCCTTAACCAC R: GGTAGTAGGAGGTATCTGCGG	95, 56, 72 1 m, 45 s, 1 min
HNF4	F: CTGCTCGGAGCCACAAAGAGATCCATG R: ATCATCTGCCACGTGATGCTCTGCA	95, 58, 72 45 s, 30 s, 1 min
Albumin	F: AGTTTGCAGAAGTTTCCAAGTTAGTG R: AGGTCCGCCCTGTCATCAG	95, 55, 72 45 s, 30 s, 1 min
Apolipoprotein-a	F:AGGCTCGGCATTTCTGGCAG R: TATCCCAGAACTCCTGGGTC	95, 55, 72 45 s, 30 s, 1 min
HTF	F: TCGCTACAGCCTTTGCAATG R: TTGAGGGTACGGAGGAGTTCC	95, 55, 72 45 s, 30 s, 1 min
E-cadherin	F: TCCATTTCTTGGTCTACGCC R: TTTGTCCTACCGACTTCCAC	95, 55, 72 45 s, 30 s, 1 min
CYP 1B1	F: CACCAAGGCTGAGACAGTGA R: GCCAGGTAAACTCCAAGCAC	94, 57, 72 30 s, 30 s, 1 min
CYP 2C9	F: GGACAGAGACGACAAGCACA R: TGGTGGGGAGAAGGTCAAT	94, 57, 72 30 s, 30 s, 1 min
CYP 2B	F: GGCACACAGCCAAGTTTACA R: CCAGCAAAGAAGAGCGAGAG	94, 57, 72 30 s, 30 s, 1 min
CYP 3A4	F: TGTGCCTGAGAACACCAGAG R: GCAGAGGAGCCAAATCTACC	94, 57, 72 30 s, 30 s, 1 min
CYP 2E1	F: CCGCAAGCATTTTGACTACA R: GCTCCTTCACCCTTTCAGAC	94, 57, 72 30 s, 30 s, 1 min
CYP 1A1	F: AGGCTTTTACATCCCCAAGG R: GCAATGGTCTCACCGATACA	94, 57, 72 30 s, 30 s, 1 min
GAPDH	F: CCATGGAGAAGGCTGGGG R: CAAAGTTGTCATGGATGACC	95, 8, 72 45 s, 30 s, 1 min

Table 1 (*continued*)

Genes	Primer sequence 5′–3′	PCR parameters[a]
CD81	F: CTCAACTGTTGTGGCTCCAAC R: CCAATGAGGTACAGCTTCCC	95, 55, 72 45 s, 30 s, 1 min
TLR3	F: GATCTGTCTCATAATGGCTTG R: GACAGATTCCGAATGCTTGTG	95, 55, 72 45 s, 30 s, 1 min
TLR7	F: CCAGACATCTCCCCAGCGTC R: GGCAAAACAGTAGGGACGGC	95, 55, 72 45 s, 30 s, 1 min
TLR8	F: CTGTGAGTTATGCGCCGAAG R: CGGGATTTCCGTTCTGGTGC	95, 55, 72 45 s, 30 s, 1 min
Myd88	F: GGTCTCCTCCACATCCTCCC R: CCAGCTTGGTAAGCAGCTCG	95, 55, 72 45 s, 30 s, 1 min
IRF3	F: GAACCCCAAAGCCACGGATC R: CCTCCCGGGAACATATGCAC	95, 55, 72 45 s, 30 s, 1 min
IRF7	F: GTGCTGTTCGGAGAGTGGCTC R: CAGCCCAGGCCTTGAAGATG	95, 55, 72 45 s, 30 s, 1 min

CYP, cytochrome P450; EGFR, epidermal growth factor receptor; F, forward primer; FGFR, fibroblast growth factor receptor; GAPDH, glyceraldehyde phosphate dehydrogenase; HGF, hepatocyte growth factor; HGFR, hepatocyte growth factor receptor; HNF, hepatocyte nuclear factor; HTF, human transferrin; IGF-1R, insulin-like growth factor-type I receptor; IRF, interferon regulatory factor; R, reverse primer; TGF, transforming growth factor; TGFR, transforming growth factor receptor; TLR, toll like receptor.

[a] Temperatures are tabulated in the first lane in degrees celsius and the corresponding times in the second lane. Performing one-step RT-PCR, reverse transcription was carried out at 42 °C for 20 min with a pre-PCR denaturation at 95 °C for 10 min.

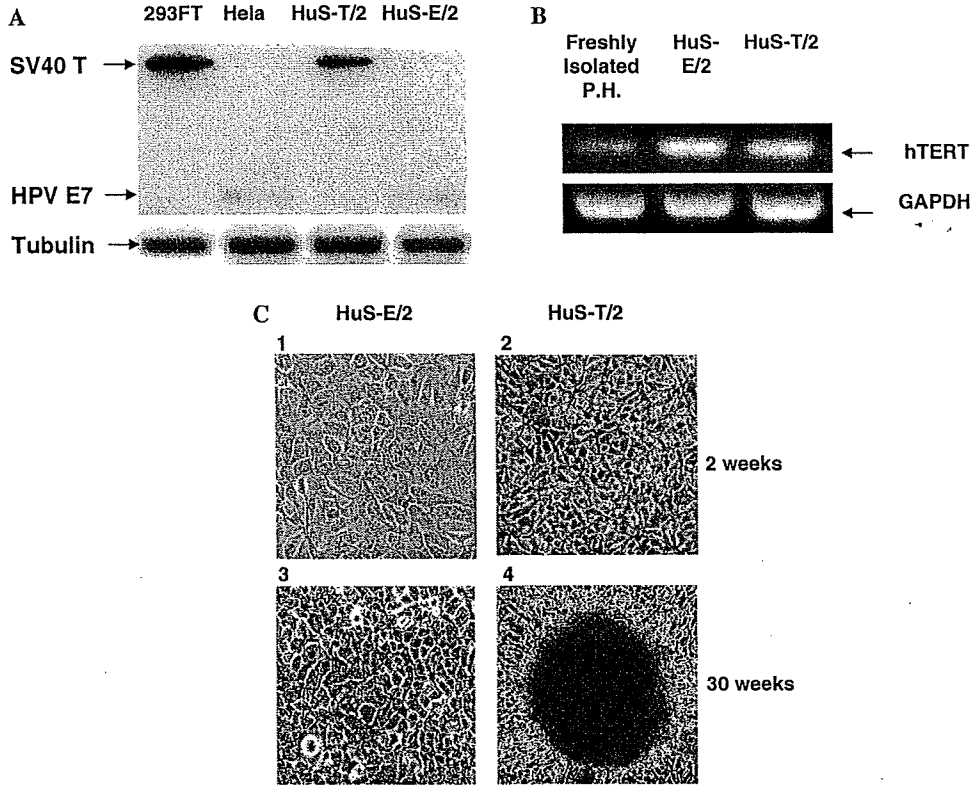

Fig. 1. (A) Immunoblot detection of SV40 T and HPV E7 expression in HuS-T/2 and HuS-E/2 cells, respectively. 293-FT and HeLa cells were used as positive controls for SV40 T and HPV E7 expression, respectively. The specific bands representing the targets are indicated. Detection of tubulin expression in all cells served as an internal control. (B) Human Telomerase Reverse Transcriptase (hTERT) expression was examined by RT-PCR in freshly isolated hepatocytes and the HuS-E/2 and HuS-T/2 cell lines. GAPDH expression was used as an internal control. The hTERT-specific bands are shown. (C) Morphological characteristics of HuS-E/2 and HuS-T/2 cells after two (panels 1 and 2) and 30 (panels 3 and 4) weeks in culture. [This figure appears in colour on the web.]

while the HPV18/E6E7-immortalized clones were named HuS-E cells and given numbers from 1 to 4. Expression of SV40 T and HPV E7 proteins was detected in the appropriate cells by immunoblot analysis (Fig. 1A). In both immortalized cell lines, expression of hTERT-mRNA was enhanced in comparison to non-transduced, freshly isolated hepatocytes as determined by RT-PCR (Fig. 1B). HuS-E cells were larger in size and exhibited slower growth than HuS-T cells (Fig. 1C).

3.2. Characterization of HuS-E and HuS-T immortalized hepatocytes

The HuS-E/2 and HuS-T/2 clones demonstrated the highest expression of hepatocyte-specific markers and transcription factors by RT-PCR (data not shown); these cells were used as representative for each group in this study. To address if HuS-E/2 and HuS-T/2 maintained similar characteristics as primary hepatocytes, they were both cultured continuously for 30 weeks and the expression profiles of a variety of growth factors (Fig. 2A), growth factor receptors (Fig. 2B), hepatocyte-specific nuclear factors (Fig. 2C), albumin, apolipoprotein-A1, transferrin (Fig. 2D), cytochrome p450 (CYP) genes (Fig. 2E), and GAPDH were compared with freshly isolated primary hepatocytes after isolation or two weeks of culture, Huh-7.5 cells, and 293 cells. After two weeks in culture, the expression of nearly all examined genes was similar between freshly isolated hepatocytes and the HuS-E/2 cell line. HuS-E/2 cells, however, exhibited higher expression of TGFβ2 (Fig. 2A), TGFβ2R, and HGFR (Fig. 2B) and lower expression of CYP 3A4 and 2C9 (Fig. 2E) in comparison to freshly isolated hepatocytes. Primary hepatocytes displayed reduced expression of TGFβ1 and TGFβ2 (Fig. 2A) and a loss of CYP1A1 expression (Fig. 2E) after two weeks of culture. HuS-E/2 cells exhibited higher expression of HGF (Fig. 2A), HGF receptor (Fig. 2B), HNF-4, (Fig. 2C), albumin, apolipoprotein-A1, HTF, and E-cadherin (Fig. 2D) in comparison to HuS-T/2 cells. Expression of CYP 3A4 (Fig. 2E) was lost from both HuS-T/2 and HuS-E/2 cells, while HuS-T/2 cells also lost the expression of HNF-1α (Fig. 2D), and CYPs 2B, 2E1 (Fig. 2E).

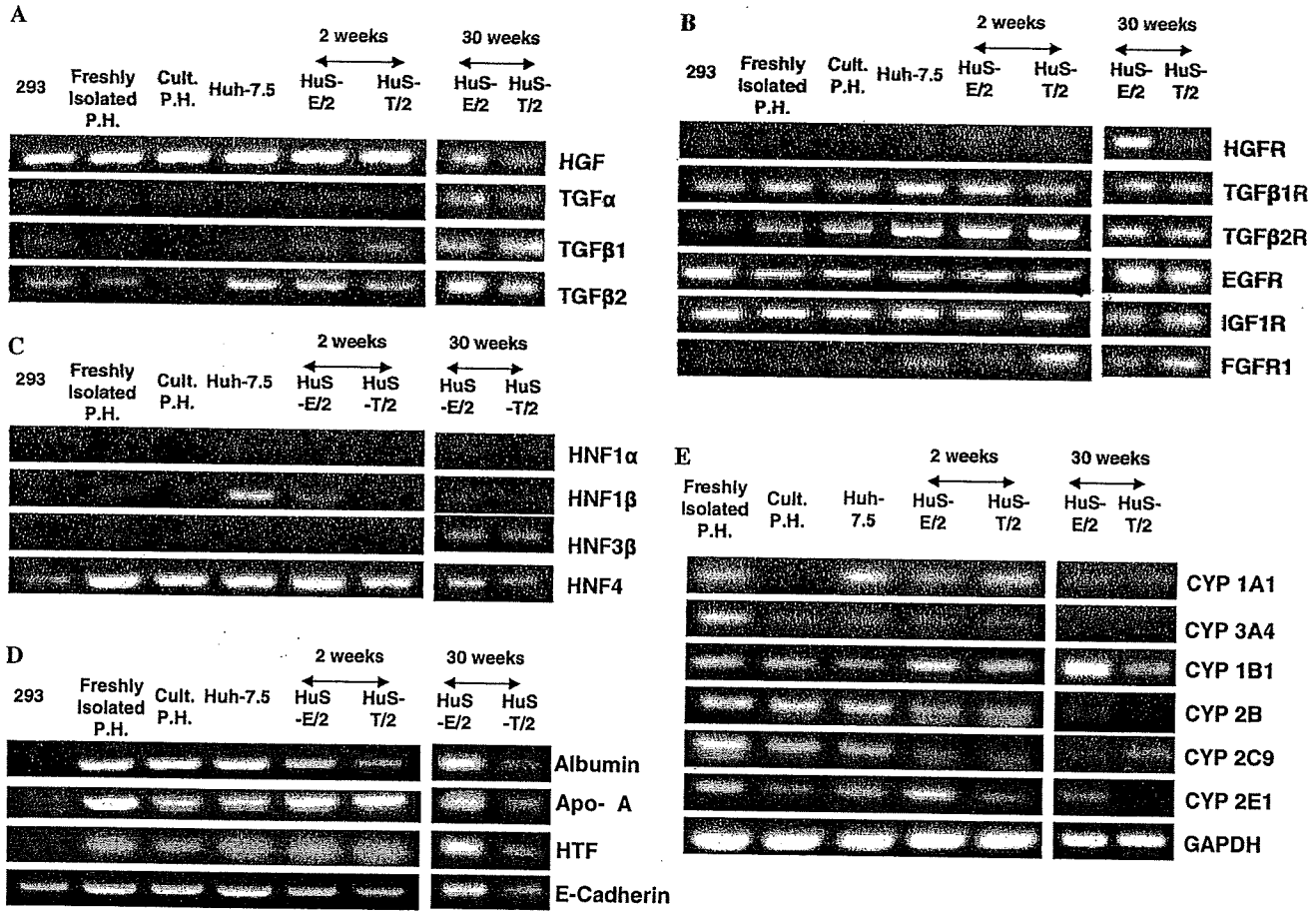

Fig. 2. Expression of the genes encoding growth factors (A), growth factor receptors (B), hepatocyte-specific nuclear factors (C), hepatocyte differentiation and functional markers (D), and CYP enzymes (E) in 293 cells, freshly isolated primary hepatocytes (P.H.), primary hepatocytes cultured for two weeks (Cult. P.H.), Huh-7.5 cells, and HuS-E/2 and HuS-T/2 cells cultured for two and 30 weeks were investigated by RT-PCR. The bands representing specific targets are indicated in the representative reactions.

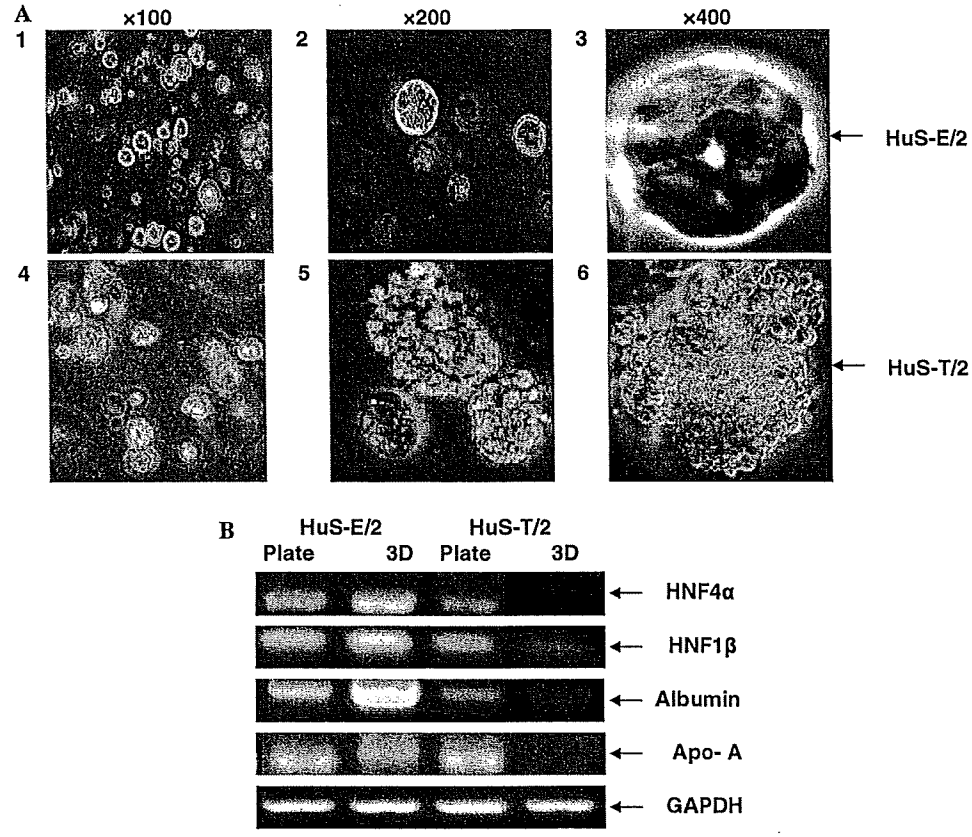

Fig. 3. (A) The morphology of HuS-E/2 and HuS-T/2 cells in 3D culture. HuSE/2 and HuS-T/2 cells were cultured in Mebiol Gel in 12-well plates at a concentration of 5×10^5 cells/well. The microscopic characteristics of these cells after one week of 3D culture are shown. (B) The expressions of HNF4α, HNF1β, albumin, and apo-A by HuS-E/2 and HuS-T/2 cells in both flat and 3D cultures are detailed. After one week of culture of HuS-E/2 and HuS-T/2 cells in flat and 3D cultures, the expressions of HNF4α, HNF1β, albumin, and apo-A were measured by RT-PCR in 250 ng total RNA.

HuS-T/2 but not in HuS-E/2 cells showed a transformed-like character starting from the 13th week of culture. This was demonstrated by continuing proliferation after confluence, pile-up formations (Fig. 1C), and proliferating in serum-deprevied condition. However, HuS-E/2 cells did not show any transformed-like characters even after 30 weeks of culture.

3.3. The characteristics of HuS-E and HuS-T immortalized hepatocytes in 3D culture

After one week in 3D culture, HuS-E/2 (Fig. 3A, panels 1, 2, and 3) cells adopted a donut-shaped structure with a central pore, while HuS-T/2 cells (Fig. 3A, panels 4, 5, and 6) displayed irregular mass formations (similar to the growth pattern of Huh-7.5 cells in 3D culture (data not shown)). In 3D culture, while the expression of HNF4, HNF1β, and albumin was enhanced in HuS-E/2, it was decreased in HuS-T/2 cells (Fig. 3B).

3.4. HCV infection to HuS-E/2

We further assessed the HCV infectivity of HuS-E- and HuS-T-derived clones by infection with HCV-1b-infected serum. Of the three HuS-E clones examined, HuS-E/2 clone demonstrated the highest infectability with HCV genotype 1b in comparison to Huh-7.5, PH5CH8 (Fig. 4A), and HuS-T cells (data not shown), which were excluded from further experiments.

3.5. Anti-CD81 blocked HCV infectivity

CD81 is involved in the entry of HCV pseudoparticles [24] and in vitro-synthesized JFH-1 [7]. To determine if authentic viral particles follow the same route of entry when infecting HuS-E/2 cells, we first examined the CD81 expression by RT-PCR. Both HuS-E/2 and HuS-T/2 cells expressed similar amounts of CD81 as freshly isolated hepatocytes and Huh-7.5 cells (Fig. 4B). Antibodies against CD81 reduced HCV infectivity of HuS-E/2 cells from the levels seen using a non-specific control antibody, confirming the importance of CD81 in HCV infectivity (Fig. 4C).

3.6. IFNα blocked HCV infectivity

We treated HuS-E/2 cells with HCV-containing serum. Cells were then cultured in fresh medium supplemented

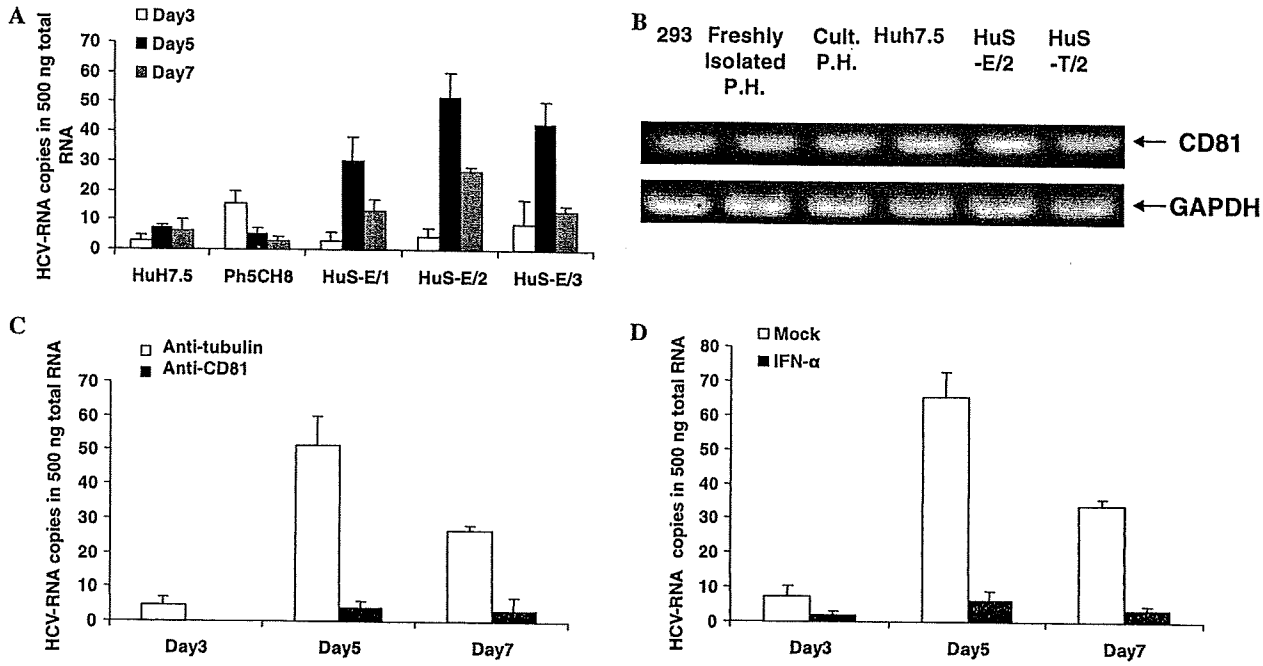

Fig. 4. (A) Serum from an HCV patient was used to infect Huh-7.5 cells, PH5CH8 cells, and three HPV E6E7-immortalized clones (HuS-E/1-3) for 24 h. After washing three times in phosphate-buffered saline (PBS), cells were cultured in fresh medium. Cells were then harvested and lysed at the indicated time points. The quantity of HCV genome RNA per 500 ng total RNA was determined by real-time RT-PCR analysis. (B) HuS-E/2 and HuS-T/2 cells both expressed CD81. Expression of CD81 (upper panel) and GAPDH as an internal control (lower panel) in 293 cells, freshly isolated P.H., cultured P.H., and Huh-7.5, HuS-E/2, and HuS-T/2 cells was investigated by RT-PCR. (C) Anti-CD81 antibodies blocked HCV infectivity. HCV infection was performed as described in (A) with the addition of CD81-specific (black bar) or anti-tubulin antibodies (control, white bar). (D) IFNα inhibits HCV multiplication in HuS-E/2 cells infected with HCV-containing serum. HuS-E/2 cells were infected with HCV as described in (A). After washing three times with PBS, cells were cultured in fresh medium supplemented with (black bar) or without (white bar) 100 U/ml IFNα.

without or with 100 U/ml IFNα. The enhancement of the HCV-RNA genome titers on the fifth day (about 10-fold) was not observed in cells treated continuously with IFNα (Fig. 4D). This result suggests that IFNα inhibited HCV replication in infected HuS-E/2 cells.

3.7. The effect of blocking IRF-3 and IRF-7 signaling on HCV infectivity

Production of interferon-alpha (IFNα) and interferon-beta (IFNβ) limits viral replication and spread, providing one of the most effective innate antiviral responses [25]. Signaling through IRF-3 and IRF-7 plays important roles in the stimulation of IFN-α/β production [25]. To determined which molecules (IRF-3 or IRF-7) play an important role in modulation of the innate immune response against HCV infection in these cells, we first detected intrinsic expression of double-stranded RNA-stimulated Toll-like receptor (TLR) 3, the downstream effector IRF-3, single-stranded RNA-stimulated TLR7, and 8, and the downstream effectors MyD88 and IRF-7 by RT-PCR. TLR3 exhibited very low expression in freshly isolated hepatocytes, Huh-7.5, HuS-E/2, and HuS-T/2 cells, while TLR7, TLR8, MyD88, and IRF-7 were easily detectable in both freshly isolated and immortalized cell lines (Fig. 5A).

The abilities of DNIRF-3 and DNIRF-7 to inhibit IFNβ and IFNα production by HuS-E/2 cells infected with Sendai virus were confirmed using assays of IFNβ or IFNα promoter-driven luciferase reporters. DNIRF-3 exhibited strong inhibition of IFNβ production (Fig. 5B) and weaker inhibition of IFNα transcription (Fig. 5C), while DNIRF-7 strongly inhibited IFNα production (Fig. 5C) and only weakly inhibited IFNβ production (Fig. 5B).

We then assessed the inhibition of HCV infectivity by DNIRF-3 and DNIRF-7. Transient transfection with DNIRF-3, DNIRF-7, or an empty vector was performed prior to HCV infection. Using Effectene reagent, the efficiency of plasmid transfection into HuS-E/2 cells was approximately 70% (data not shown). While there was no significant effect of DNIRF-3 on HCV infectivity, DNIRF-7 demonstrated a marked increase in HCV titers on days 3 and 5 after infection in comparison to control cells (Fig. 5D). To confirm that the enhancement of HCV replication by DNIRF-7 is not mediated by the impairment of IRF-3 signaling by heterodimeric interactions between IRF-3 and DNIRF-7, we performed siRNA inhibition of IRF-3 and IRF-7. The reduction of IRF-3 and IRF-7 expression by siRNA was obvious by RT-PCR (Fig. 5E). siRNA-mediated suppression of either IRF-3 or IRF-7 inhibited IFNβ and IFNα production

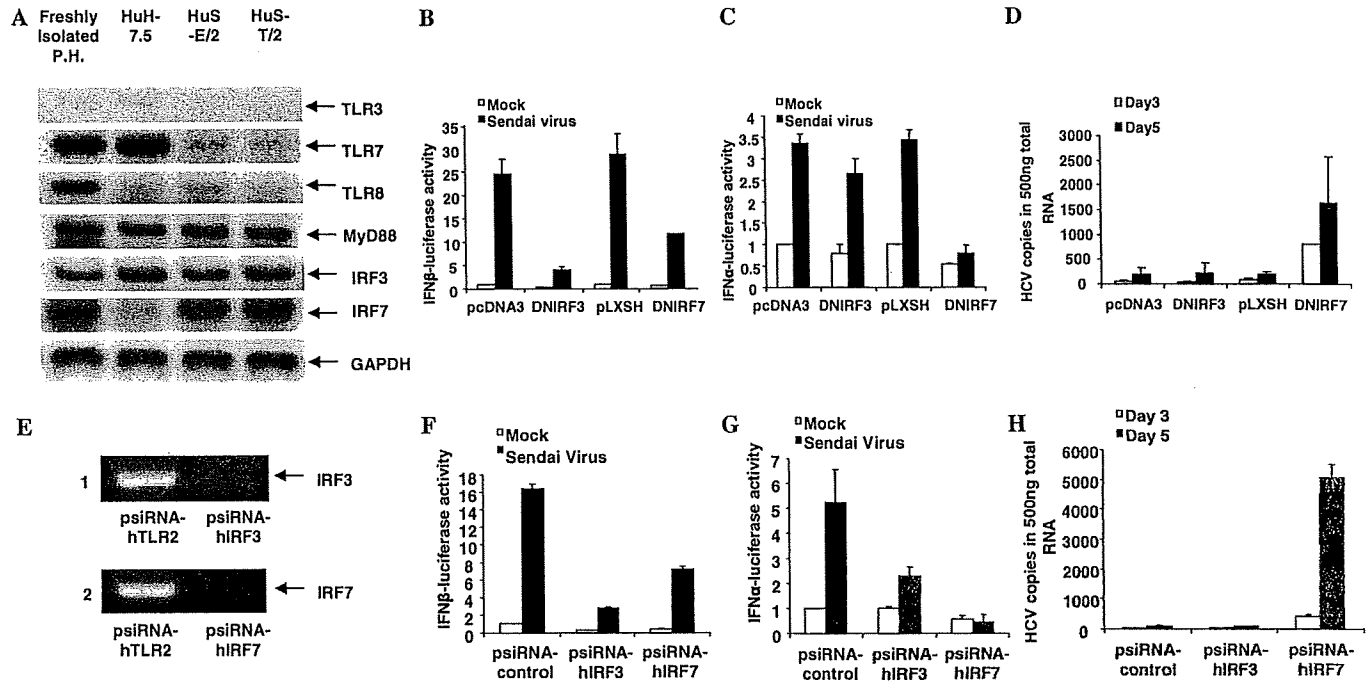

Fig. 5. (A) We examined the expression of TLR3, TLR7, TLR8, MyD88, IRF-3, and IRF-7, as well as GAPDH as an internal control in freshly isolated primary hepatocytes and Huh-7.5, HuS-E/2, and HuS-T/2 cells was investigated by RT-PCR. (B and C) HuS-E/2 cells were cotransfected with pIFNβ-luc (B) or pIFNα-luc (C) with an expression plasmid encoding DNIRF-3, DNIRF-7, or the appropriate empty vector (pcDNA3 and PLXSH, respectively). Twenty-four hours later, cells were infected (black bar) with Sendai virus or mock-infected (white bar), then analyzed for luciferase activity after 12 h. (D) IRF-7, but not IRF-3, suppression enhanced HCV infectivity of HuS-E/2 cells. HuS-E/2 cells were transiently transfected with empty pcDNA3, DNIRF-3, empty pLXSH, or DNIRF-7 plasmids. Twenty-four hours later, serum from a patient with HCV was used to infect transfected cells for 24 h. After washing, cells were cultured in fresh medium. The cells were then harvested and lysed at the indicated time points. The quantity of HCV genome RNA per 500 ng total RNA was determined by real-time RT-PCR analysis. (E) IRF-3 and IRF-7 levels were suppressed by specific siRNAs. HuS-E/2 cells were transfected with control psiRNA-hTLR2, psiRNA-hIRF-3, or psiRNA-hIRF-7, then selected with Zeocin at 250 μg/ml. Two weeks later, cells were harvested and assessed for the expression of IRF-3 and IRF-7 by RT-PCR. (F and G) HuS-E/2 cells were transfected with control psiRNA-hTLR2, psiRNA-hIRF-3, or psiRNA-hIRF-7, followed by selection in Zeocin at 250 μg/ml. Two weeks later, cells were cotransfected with pIFNβ-luc (F) or pIFNα-luc (G). Twenty-four hours later, cells were infected (black bar) with Sendai virus or mock-infected (white bar), then analyzed for luciferase activity after 12 h. (H) Transfected cells were infected with serum from HCV patient; HCV infectivity was assessed as described above.

in HuS-E/2 cells infected with Sendai virus in patterns similar to the effects seen following DNIRF-3 and DNIRF-7 expression, respectively (Figs. 5F and G). Blockade of IRF-7 expression resulted in a significantly higher titer of HCV after infection, while IRF-3 down-regulation did not have any significant effect on HCV titers (Fig. 5H). The enhancement of IRF-7 silencing by siRNA improved the infectivity of HCV (data not shown). These results suggest that IRF-7 plays the major role in the innate immune response to HCV in HuS-E/2 cells.

3.8. Establishment of stable DNIRF-7 expressing clones derived from HuS-E/2 cells

Since DNIRF-7 enhanced HCV infectivity, we transduced the plasmid encoding DNIRF-7 and a hygromycin-B resistance gene, into HuS-E/2 cells. Following selection with hygromycin-B, we obtained the HuS-E7/DN22 and HuS-E7/DN24 clones. As detected by RT-PCR, both clones demonstrated similar expression levels of albumin, apolipoprotein-A1, and HNF4 as the parental HuS-E/2 cells (Fig. 6A). The HuS-E7/DN24 clone exhibited stronger expression of DNIRF-7 than the HuS-E7/DN22 clone by immunoblotting (Fig. 6B). The induction of IFNα in HuS-E7/DN24 in response to infection with an RNA virus (Sendai virus) was low in comparison to the parental HuS-E/2 and HuS-E7/DN22 clones, as detected by IFNα-luciferase reporter assay (Fig. 6C). HuS-E7/DN24 also exhibited a higher HCV infectability in comparison to parental HuS-E/2 cells and the HuS-E7/DN22 clone (Fig. 6D).

3.9. Infection of HuS-E7/DN24 cells with different HCV genotypes

Huh7.5 and HuS-E7/DN24 cells were separately infected with serums derived from 3 different HCV-patients or by JFH-1 concentrated medium (HCV-2a). Two serums were infected by HCV-1b, while the third by HCV-2b. Inoculated virus titer was adjusted to be the same in all cases. Except for JFH-1, which efficiently

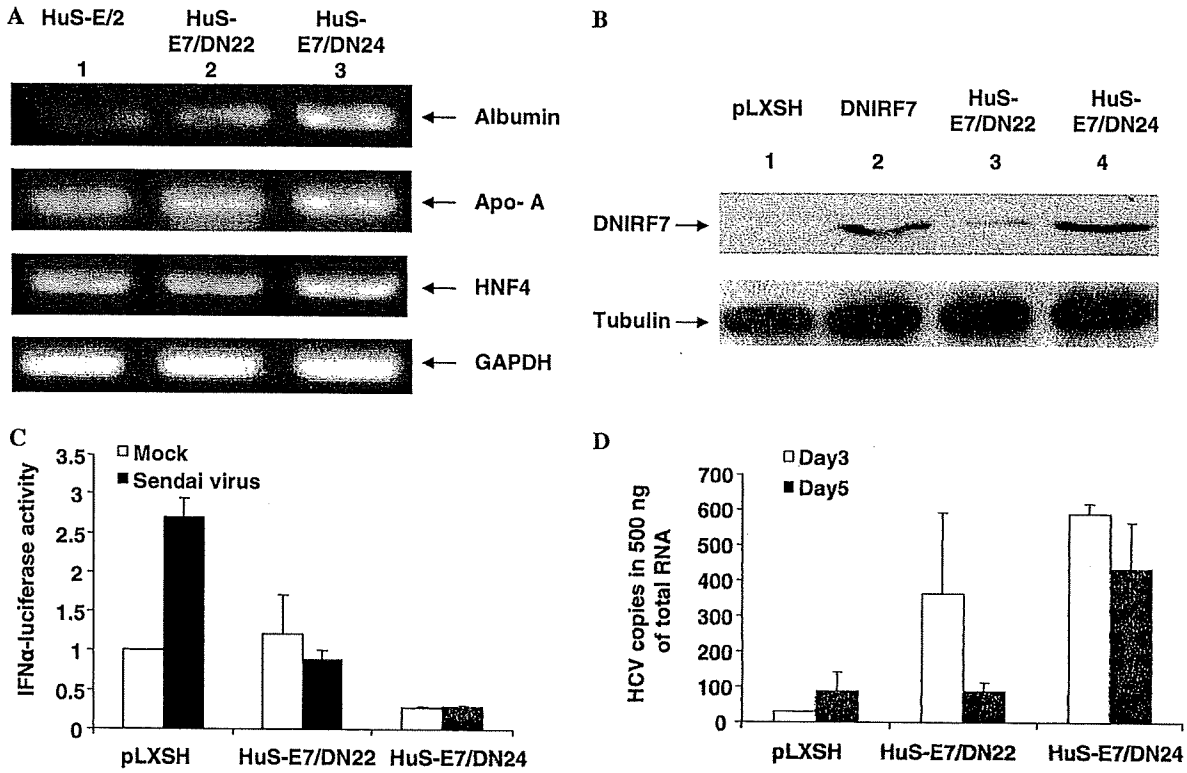

Fig. 6. (A) The pLXSH-HA-DNIRF-7 plasmid was transfected into HuS-E/2 cells, followed by selection in 100 μg/ml Hygromycin B. Two clones, HuS-E7/DN22 (lane 2) and HuS-E7/DN24 (lane 3), were obtained. We investigated the expression of albumin, apo-A, HNF4, and GAPDH as an internal control in parental HuS-E/2, HuS-E7/DN22, and HuS-E7/DN24 hepatocytes cultured for two weeks by RT-PCR. (B) Expression of HA-tagged DNIRF-7 (upper panel) and tubulin (control, lower panel) was detected by immunoblotting analysis. HuS-E/2 cells transiently transfected with either empty pLXSH vector (lane 1) or pLXSH-HA-DNIRF-7 (lane 2) were used as negative and positive controls, respectively, after 48 h. (C) HuS-E/2, HuS-E7/DN24, and HuS-E7/DN22 cells were transfected with IFNα-luc. HuS-E/2 cells were also cotransfected with pLXSH. All of these cells were then infected (black bar) or with Sendai virus or mock-infected, then analyzed for luciferase activity after 12 h. (D) HuS-E7/DN24 cells exhibited high infectivity to HCV samples derived from patient serum. HuS-E/2 cells were transiently transfected with empty pLXSH. Twenty-four hours later, serum from a recurrently transplanted HCV patient was used to infect transfected cells and HuS-E7/DN22 and HuS-E7/DN24 cells for 24 h. After washing three times, cells were cultured in fresh medium. Cells were then harvested and lysed at the indicated time points.

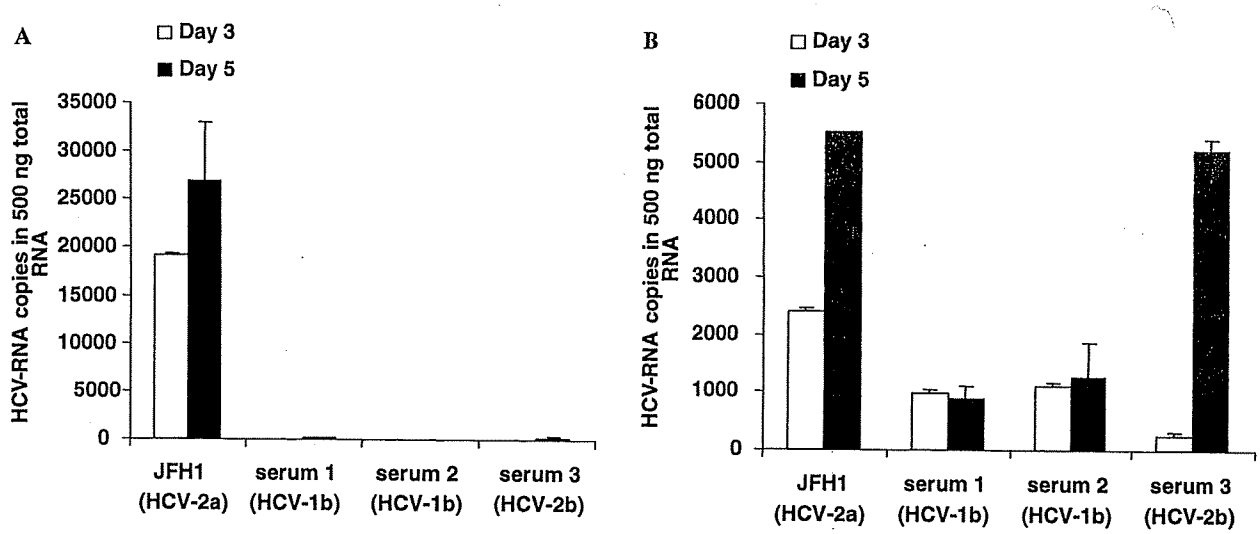

Fig. 7. The infectability of Huh-7.5 and HuS-E7/DN24 cells to different HCV genotypes. Huh-7.5 (A) and HuS-E7/DN24 (B) cells were infected with same titer of JFH1 (HCV-2a), two different HCV-1b serums and one HCV-2b serum. After removing the infected medium, the cells were washed in PBS and recultured in fresh medium. Cells were harvested and lysed at the indicated time points. The quantity of HCV genome RNA per 500 ng RNA was detected by real-time RT-PCR analysis.

replicated in Huh7.5 cells (Fig. 7A), HuS-E7/DN24 cells showed a higher and reproducible infectability for the different HCV strains than Huh7.5 cells (Fig. 7B). Similar higher infectability of HuS-E7/DN24 cells was observed with HCV-4a genotype (unpublished data). These results suggest that the high infectability of Huh-7.5 with JFH-1 is specific among the combinations of HCV strains and cell lines; while HuS-E7/DN24 cells were generally permissive to HCV-infected serum independent of HCV strains.

4. Discussion

This study demonstrates that ectopic expression of the HPV18/E6E7 genes in combination with hTERT could efficiently immortalize mature human hepatocytes, generating a cell line with stable expression of hepatocyte markers and functions for more than 30 weeks in culture. HuS-E/2 cells continuously exhibited higher expression of both HGF and HGFR than HuS-T/2 cells. This result suggests that HPV18/E6E7-immortalized hepatocytes maintain responsiveness to paracrine signals capable of inducing cell differentiation to a greater extent than SV40 T-immortalized hepatocytes. This conclusion is further supported by the increased expression of HNF4 in HuS-E/2 cells in comparison to HuS-T/2 cells. HNF4 is a major hepatocyte transcription factor, required for hepatocyte differentiation and liver-specific gene expression [26]. HNF4 drives hepatocytes differentiation by acting upstream in a transcription factor cascade that included HNF1α [27]. HuS-E/2 cells continued to express HNF1α throughout prolonged culture, while HuS-T/2 cells lost expression completely. Maintenance of hepatocellular functions was demonstrated by continuous and high expression of albumin, apolipoprotein-A, human transferrin, and E-cadherin by HuS-E/2 in comparison to HuS-T/2 cells. These differences became more pronounced in the late passages. In a similar manner, HuS-E/2 cells continued to express all of the examined CYP genes, with the exception of CYP 3A4, while HuS-T/2 cells lost expression of CYP 3A4, 1B, and 2E1 completely and displayed markedly lower expression of CYP 1B1 than HuS-E/2 cells. Thus, human hepatocytes immortalized by HPV E6/E7 transfection are phenotypically similar to primary hepatocytes, even during extended cultures.

Recently, it was reported that the JFH-1 strain and derived chimeras could only infect and propagate efficiently in Huh7.5.1 and Huh7.5 cells, both of which are subclones of Huh7 cells [7–9]. This limitation, however, may be specific to the JFH-1 **strain**, which may not accurately reflect the course of other HCV strains' infection. Thus, usage of HCV particles isolated from patient serum could be more useful to study authentic HCV infection. Using sera from HCV patients as a source of infective virus, HPV18/E6E7-immortalized cell lines exhibited higher reproducible susceptibility to HCV infection than HuS-T, PH5CH8, and Huh-7.5 cell lines.

IRF3 and IRF7 play an important role in the activation of interferon signaling [28]. We suppressed the functions of IRF-3 or IRF-7 to assess their role in HCV infectivity. In fact, we observed significant increase of HCV replication in HuS-E/2 cells bearing dominant-negative IRF7 that impaired IFN signaling. The suppression of IRF-3, however, did not have any significant effect on HCV infectivity or replication in this cell line. This may result from the blockade of IRF-3 activation by an HCV NS3/4A serine protease [29] through at least two independent pathways that inhibit the TLR3-dependent and RIG-I-dependent signaling pathways [29–33]. Although HCV was shown to inhibit basal expression levels of IRF-7 at both mRNA and protein levels and it was shown that NS5A suppresses IRF-7-induced IFNα promoter activation [34], Stimulation of TLR7 was shown to activate IRF-7 and induce suppression of HCV replicon levels in Huh-7 cells [35]. This suggests that the inhibition of IRF7 by HCV is not complete. Using IRF-7-deficient (IRF-7−/−) mice, Honda [36] demonstrated that the transcription factor IRF-7 is essential for the induction of IFNα/β genes. We established a clone stably expressing DNIRF-7 (HuS-7E/DN24), which demonstrated higher infectivity with different HCV strains than the parental HuS-E/2 clone.

In summary, we have established a human hepatocyte-derived cell line that maintains the characteristic features of primary hepatocytes by transduction with HPV18/E6E7. This cell line is highly infectable by HCV, which suggests that these cells may be useful to characterize the molecular mechanisms involved with HCV infection and to develop novel HCV treatment modalities.

Acknowledgements

We thank Dr. Akagi at Osaka Bioscience Institute for providing hTERT expressing vector, Dr. Sakai at the Institute for Virus Research, Kyoto University, for providing HPV18/E6E7 expressing plasmid, and Dr. Taniguchi of the University of Tokyo for providing IFNβ, and IFNα promoters' reporter plasmids. This work was supported by Grants-in-Aid for cancer research and for the second-term comprehensive 10-year strategies for cancer control from the Ministry of Health, Labor and Welfare, by Grants-in-Aid for scientific research from the Ministry of Education, Culture, Sports, Science and Technology, by Grants-in-Aid for the research for the future program from the Japanese society for the Promotion of Science. Dr. Hussein H. Aly is a receiver of the Japanese *Gakushu Shoreihi* scholarship and was partly supported by Prof. *Yassin A. El Ghaffar memorial scholarship* for the Improvement of Liver research in Egypt.

References

[1] Wasley A, Alter MJ. Epidemiology of hepatitis C: geographic differences and temporal trends. Semin Liver Dis 2000;20:1–16.

[2] Manns MP, McHutchison JG, Gordon SC, Rustgi VK, Shiffman M, Reindollar R, et al. Peginterferon alfa-2b plus ribavirin compared with interferon alfa-2b plus ribavirin for initial treatment of chronic hepatitis C: a randomised trial. Lancet 2001;358:958–965.

[3] Fried MW, Shiffman ML, Reddy KR, Smith C, Marinos G, Goncales Jr FL, et al. Peginterferon alfa-2a plus ribavirin for chronic hepatitis C virus infection. N Engl J Med 2002;347: 975–982.

[4] Hadziyannis SJ, Sette Jr H, Morgan TR, Balan V, Diago M, Marcellin P, et al. Peginterferon-alpha2a and ribavirin combination therapy in chronic hepatitis C: a randomized study of treatment duration and ribavirin dose. Ann Intern Med 2004;140:346–355.

[5] Muir AJ, Bornstein JD, Killenberg PG. Peginterferon alfa-2b and ribavirin for the treatment of chronic hepatitis C in blacks and non-Hispanic whites. N Engl J Med 2004;350:2265–2271.

[6] Falck-Ytter Y, Kale H, Mullen KD, Sarbah SA, Sorescu L, McCullough AJ. Surprisingly small effect of antiviral treatment in patients with hepatitis C. Ann Intern Med 2002;136:288–292.

[7] Wakita T, Pietschmann T, Kato T, Date T, Miyamoto M, Zhao Z, et al. Production of infectious hepatitis C virus in tissue culture from a cloned viral genome. Nat Med 2005;11:791–796.

[8] Zhong J, Gastaminza P, Cheng G, Kapadia S, Kato T, Burton DR, et al. Robust hepatitis C virus infection in vitro. Proc Natl Acad Sci USA 2005;102:9294–9299.

[9] Lindenbach BD, Evans MJ, Syder AJ, Wolk B, Tellinghuisen TL, Liu CC, et al. Complete replication of hepatitis C virus in cell culture. Science 2005;309:623–626.

[10] Dellgado JP, Parouchev A, Allain JE, Pennarun G, Gauthier LR, Dutrillaux AM, et al. Long-term controlled immortalization of a primate hepatic progenitor cell line after Simian virus 40 T-Antigen gene transfer. Oncogene 2005;24:541–551.

[11] Mizuguchi T, Mitaka T, Katsuramaki T, Hirata K. Hepatocyte transplantation for total liver repopulation. J Hepatobiliary Pancreat Surg 2005;12:378–385.

[12] Isom HC, Tevethia MJ, Kreider JW. Tumorigenicity of simian virus 40-transformed rat hepatocytes. Cancer Res 1981;41: 2126–2134.

[13] Ray FA, Waltman MJ, Lehman JM, Little JB, Nickoloff JA, Kraemer PM. Identification of SV40 T-antigen mutants that alter T-antigen-induced chromosome damage in human fibroblasts. Cytometry 1998;31:242–250.

[14] Chen WH, Lai WF, Deng WP, Yang WK, Lo WC, Wu CC, et al. Tissue engineered cartilage using human articular chondrocytes immortalized by HPV-16 E6 and E7 genes. J Biomed Mater Res A 2006;76:512–520.

[15] Dimri G, Band H, Band V. Mammary epithelial cell transformation: insights from cell culture and mouse models. Breast Cancer Res 2005;7:171–179.

[16] Harms W, Rothamel T, Miller K, Harste G, Grassmann M, Heim A. Characterization of human myocardial fibroblasts immortalized by HPV16 E6–E7 genes. Exp Cell Res 2001;268:252–261.

[17] Shiga T, Shirasawa H, Shimizu K, Dezawa M, Masuda Y, Simizu B. Normal human fibroblasts immortalized by introduction of human papillomavirus type 16 (HPV-16) E6-E7 genes. Microbiol Immunol 1997;41:313–319.

[18] Akimov SS, Ramezani A, Hawley TS, Hawley RG. Bypass of senescence, immortalization, and transformation of human hematopoietic progenitor cells. Stem Cells 2005;23:1423–1433.

[19] Hung SC, Yang DM, Chang CF, Lin RJ, Wang JS, Low-Tone Ho L, et al. Immortalization without neoplastic transformation of human mesenchymal stem cells by transduction with HPV16 E6E7 genes. Int J Cancer 2004;110:313–319.

[20] Wang G, Johnson GA, Spencer TE, Bazer FW. Isolation, immortalization, and initial characterization of uterine cell lines: an in vitro model system for the porcine uterus. In vitro Cell Dev Biol Anim 2000;36:650–656.

[21] Hino H, Tateno C, Sato H, Yamasaki C, Katayama S, Kohashi T, et al. A long-term culture of human hepatocytes which show a high growth potential and express their differentiated phenotypes. Biochem Biophys Res Commun 1999;256:184–191.

[22] Watashi K, Hijikata M, Hosaka M, Yamaji M, Shimotohno K. Cyclosporin A suppresses replication of hepatitis C virus genome in cultured hepatocytes. Hepatology 2003;38:1282–1288.

[23] Murata T, Ohshima T, Yamaji M, Hosaka M, Miyanari Y, Hijikata M, et al. Suppression of hepatitis C virus replicon by TGF-beta. Virology 2005;331:407–417.

[24] Dasgupta A, Hughey R, Lancin P, Larue L, Moghe PV. E-cadherin synergistically induces hepatospecific phenotype and maturation of embryonic stem cells in conjunction with hepatotrophic factors. Biotechnol Bioeng 2005;92:257–266.

[25] Civas A, Island ML, Genin P, Morin P, Navarro S. Regulation of virus-induced interferon-A genes. Biochimie 2002;84:643–654.

[26] Ishiyama T, Kano J, Minami Y, Iijima T, Morishita Y, Noguchi M. Expression of HNFs and C/EBP alpha is correlated with immunocytochemical differentiation of cell lines derived from human hepatocellular carcinomas, hepatoblastomas and immortalized hepatocytes. Cancer Sci 2003;94:757–763.

[27] Wege H, Le HT, Chui MS, Liu L, Wu J, Giri R, et al. Telomerase reconstitution immortalizes human fetal hepatocytes without disrupting their differentiation potential. Gastroenterology 2003;124: 432–444.

[28] Mamane Y, Heylbroeck C, Genin P, Algarte M, Servant MJ, LePage C, et al. Interferon regulatory factors: the next generation. Gene 1999;237:1–14.

[29] Foy E, Li K, Wang C, Sumpter Jr R, Ikeda M, Lemon SM, et al. Regulation of interferon regulatory factor-3 by the hepatitis C virus serine protease. Science 2003;300:1145–1148.

[30] Sumpter Jr R, Loo YM, Foy E, Li K, Yoneyama M, Fujita T, et al. Regulating intracellular antiviral defense and permissiveness to hepatitis C virus RNA replication through a cellular RNA helicase, RIG-I. J Virol 2005;79:2689–2699.

[31] Breiman A, Grandvaux N, Lin R, Ottone C, Akira S, Yoneyama M, et al. Inhibition of RIG-I-dependent signaling to the interferon pathway during hepatitis C virus expression and restoration of signaling by IKKepsilon. J Virol 2005;79:3969–3978.

[32] Li K, Foy E, Ferreon JC, Nakamura M, Ferreon AC, Ikeda M, et al. Immune evasion by hepatitis C virus NS3/4A protease-mediated cleavage of the Toll-like receptor 3 adaptor protein TRIF. Proc Natl Acad Sci USA 2005;102:2992–2997.

[33] Foy E, Li K, Sumpter Jr R, Loo YM, Johnson CL, Wang C, et al. Control of antiviral defenses through hepatitis C virus disruption of retinoic acid-inducible gene-I signaling. Proc Natl Acad Sci USA 2005;102:2986–2991.

[34] Zhang T, Lin RT, Li Y, Douglas SD, Maxcey C, Ho C, et al. Hepatitis C virus inhibits intracellular interferon alpha expression in human hepatic cell lines. Hepatology 2005;42:819–827.

[35] Lee J, Wu CC, Lee KJ, Chuang TH, Katakura K, Liu YT, et al. Activation of anti-hepatitis C virus responses via Toll-like receptor 7. Proc Natl Acad Sci USA 2006;103:1828–1833.

[36] Honda K, Yanai H, Negishi H, Asagiri M, Sato M, Mizutani T, et al. IRF-7 is the master regulator of type-I interferon-dependent immune responses. Nature 2005;434:772–777.

nature
cell biology

The lipid droplet is an important organelle for hepatitis C virus production

Yusuke Miyanari[1,2], Kimie Atsuzawa[3], Nobuteru Usuda[3], Koichi Watashi[1,2], Takayuki Hishiki[1,2], Margarita Zayas[4], Ralf Bartenschlager[4], Takaji Wakita[5], Makoto Hijikata[1,2] and Kunitada Shimotohno[1,2,5]

The lipid droplet (LD) is an organelle that is used for the storage of neutral lipids. It dynamically moves through the cytoplasm, interacting with other organelles, including the endoplasmic reticulum (ER)[1–3]. These interactions are thought to facilitate the transport of lipids and proteins to other organelles. The hepatitis C virus (HCV) is a causative agent of chronic liver diseases[4]. HCV capsid protein (Core) associates with the LD[5], envelope proteins E1 and E2 reside in the ER lumen[6], and the viral replicase is assumed to localize on ER-derived membranes. How and where HCV particles are assembled, however, is poorly understood. Here, we show that the LD is involved in the production of infectious virus particles. We demonstrate that Core recruits nonstructural (NS) proteins and replication complexes to LD-associated membranes, and that this recruitment is critical for producing infectious viruses. Furthermore, virus particles were observed in close proximity to LDs, indicating that some steps of virus assembly take place around LDs. This study reveals a novel function of LDs in the assembly of infectious HCV and provides a new perspective on how viruses usurp cellular functions.

Hepatitis C virus (HCV) has a plus-strand RNA genome that encodes the viral structural proteins Core, E1 and E2, the p7, and the nonstructural (NS) proteins 2, 3, 4A, 4B, 5A and 5B (refs 7, 8). NS proteins are reported to localize on the cytoplasmic side of endoplasmic reticulum (ER) membranes[9]. To elucidate the mechanisms of virus production, we used a HCV strain, JFH1, which can produce infectious viruses[10–12]. We first investigated the subcellular localization of the HCV proteins in cells that had been transfected with JFH1^{E2FL} RNA, in which a part of the hypervariable region 1 of E2 was replaced by the FLAG epitope tag (see Supplementary Information, Fig. S1, S2a–d). Core localized to the lipid droplets (LDs; Fig. 1a), as previously reported[5]. Interestingly, NS proteins were also detected around LDs in 60–90% of JFH1^{E2FL}-replicating cells (Fig. 1a, c). Similar levels of colocalization of LDs with viral proteins were observed in cells that had been transfected with chimeric HCV genomes expressing structural proteins, p7 and part of NS2 of the genotype 1b (Con1) or the genotype 1a (H77) isolate (see Supplementary Information, Fig. S1, S2e)[13]. In contrast, there was no close association between the LDs and NS proteins in cells that had been transfected with JFH1^{dC3} RNA (Fig. 1b, c), which lacked the coding region of Core (Supplementary Information, Fig. S1). NS proteins were diffusely present on the ER, suggesting that NS proteins are translocated from the ER to LDs in JFH1^{E2FL}-replicating cells in a Core-dependent manner. Importantly, there was no association between LDs and PDI, an ER marker protein, indicating that either ER membranes were absent in close proximity to LDs or that PDI was excluded from such membranes (Fig. 1c). These results were supported by western blot analysis of the LD fraction (Fig. 1d). The LD fraction contained ADRP, an LD marker, but not the ER markers Calnexin and Grp78 (data not shown), indicating that there was no ER contamination in the LD fraction. However, the LD fraction from JFH1^{E2FL}-replicating cells contained high levels of viral proteins in contrast to the LD fraction from JFH1^{dC3}-replicating cells (in which HCV proteins were virtually absent (Fig. 1d, LD fraction)), even though the expression levels of the NS proteins in whole-cell extracts were similar (Fig. 1d, whole-cell extract). About 20–45% of the total HCV proteins associated with the LDs in JFH1^{E2FL}-replicating cells (Fig. 1e). Consistent with previous reports that Core enhances the formation of LDs[14], overproduction of LDs was observed in JFH1^{E2FL}-, but not JFH1^{dC3}-replicating cells (Supplementary Information, Fig. S3a–l). Treatment of the cells with oleic acid, which enhanced the formation of LDs, did not affect either HCV protein levels or the recruitment of viral proteins to LDs in JFH1^{dC3}-replicating cells (Supplementary Information, Fig. S3m–p). Thus, the overproduction of LDs is insufficient for the recruitment of HCV proteins to LDs. To examine the ability of Core to recruit NS proteins to LDs, JFH1^{dC3}-replicating cells were transfected with a plasmid-expressing Core (Core^{Wt}) (Fig. 1f, g). NS5A accumulated around LDs (Fig. 1f, arrowheads and panel 2), as did NS3 and NS4AB (Fig. 1g), in cells expressing Core^{Wt}. The translocation of NS proteins to LDs was, however, not observed in JFH1^{dC3}-replicating cells expressing Core$^{PP/AA}$ (Fig. 1g and Supplementary Information, Fig. S2f–h),

[1]Department of Viral Oncology, Institute for Virus Research, Kyoto University, Kyoto 606-8507, Japan; [2]Graduate School of Biostudies, Kyoto University, Kyoto 606-8507, Japan; [3]Department of Anatomy, Fujita Health University School of Medicine, Toyoake 470-1192, Japan; [4]Department of Molecular Virology, University of Heidelberg, 69120 Heidelberg, Germany; [5]Department of Virology II, National Institute of Infectious Diseases, Tokyo 162-8640, Japan
[5]Correspondence should be addressed to K.S. (e-mail: shimkuni@z8.keio.jp)

Received 16 March 2007; accepted 31 July 2007; published online 26 August 2007; DOI: 10.1038/ncb1631

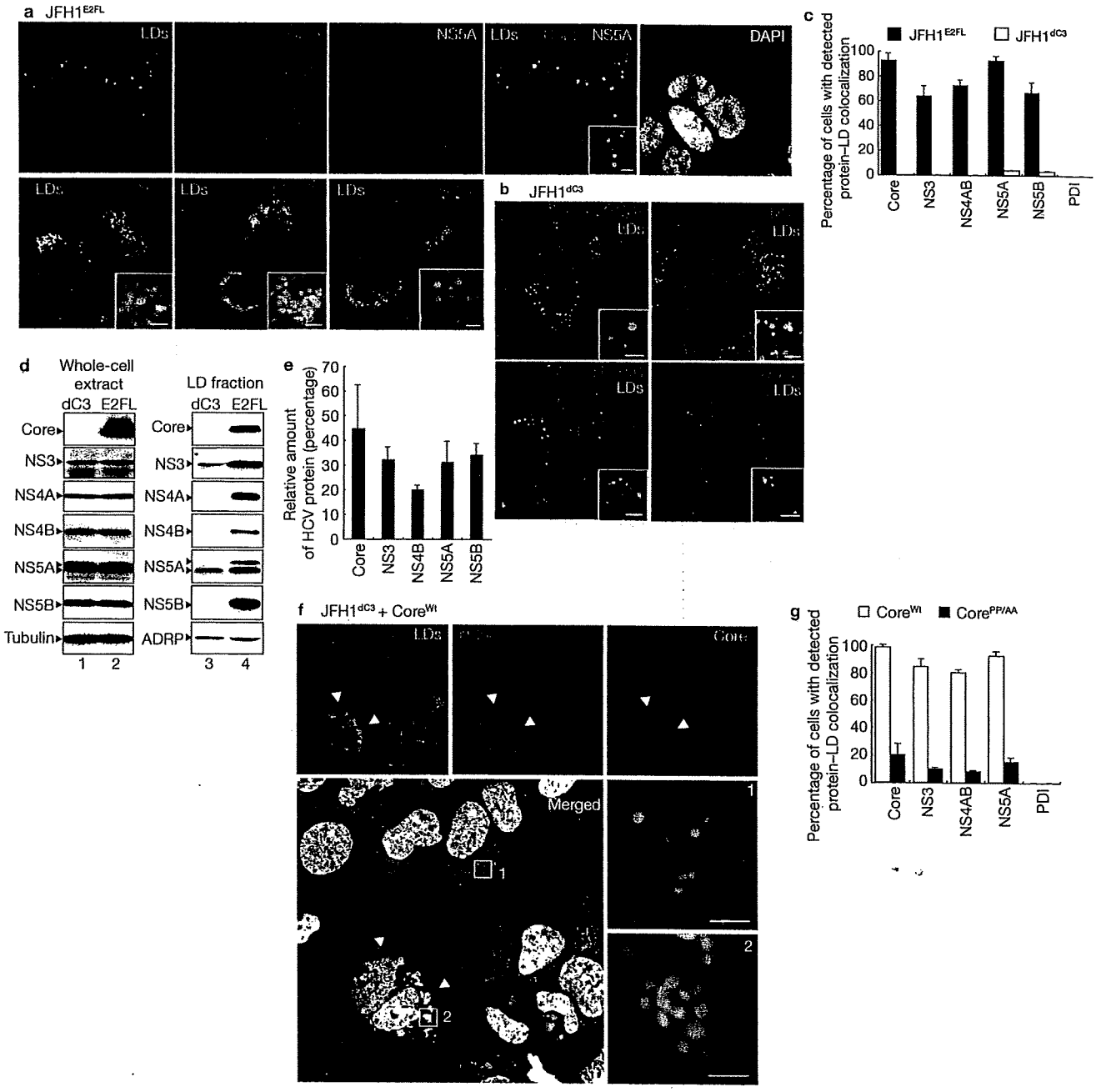

Figure 1 Core recruits NS proteins to LDs. **(a)** Huh-7 cells transfected with JFH1^{E2FL} RNA were labelled with antibodies against Core (red), NS5A (blue), NS3 (red), NS4AB (red) or NS5B (red). Lipid droplets (LDs) and nuclei were stained with BODYPI 493/503 (green) and DAPI (white in upper panel, blue in lower panels), respectively. Insets are high magnification images of areas in the respective panel. **(b)** JFH1^{dC3} replicon-bearing cells were labelled with DAPI (blue), BODIPY 493/503 (green) and indicated antibodies (red). The insets are high magnifications of the corresponding panel. **(c)** Percentages of JFH1^{E2FL}- or JFH1^{dC3}-bearing cells in which hepatitis C virus (HCV) proteins or PDI colocalize with LDs ($n > 200$). **(d)** Western blot analysis of HCV proteins and marker proteins in whole-cell extracts and the LD fractions from cells transfected with JFH1^{E2FL} (E2FL) or JFH1^{dC3} (dC3) RNA. **(e)** HCV proteins were quantified by using western blotting data of the purified LD fraction and whole-cell extracts of JFH1^{E2FL}-replicating cells. Results are shown as relative amounts of HCV proteins co-fractionated with LDs. This results correspond well with results obtained by quantitative immunofluorescence staining (data not shown). **(f)** Trans-complementation with Core^{Wt} relocates NS proteins to LDs. JFH1^{dC3} replicon-bearing cells were transfected with pcDNA3–Core^{Wt} and labelled with BODIPY 493/503 (green), DAPI (white) and antibodies against NS5A (red) and Core (blue). Arrowheads indicate Core^{Wt}-expressing cells. Higher-magnification images of area 1 and area 2 are shown in panels 1 and 2, respectively. Scale bars, 2 μm. **(g)** The percentages of cells in which HCV proteins colocalize with LDs in the presence of Core^{Wt} or Core $^{PP/AA}$ ($n > 200$). Uncropped images of gels are shown in Supplementary Information Fig. S6. All error bars are derived from s.d.

a variant of Core containing two alanine substitutions at amino-acid positions 138 and 143 that fails to associate with LDs[15]. These results show that LD-associated Core recruits NS proteins from the ER to LDs.

Next, we investigated whether Core also recruited HCV RNA to LDs. *In situ* hybridization analysis showed that in more than 80% of JFH1^{E2FL}-replicating cells, both plus- and minus-strand RNAs were diffusely

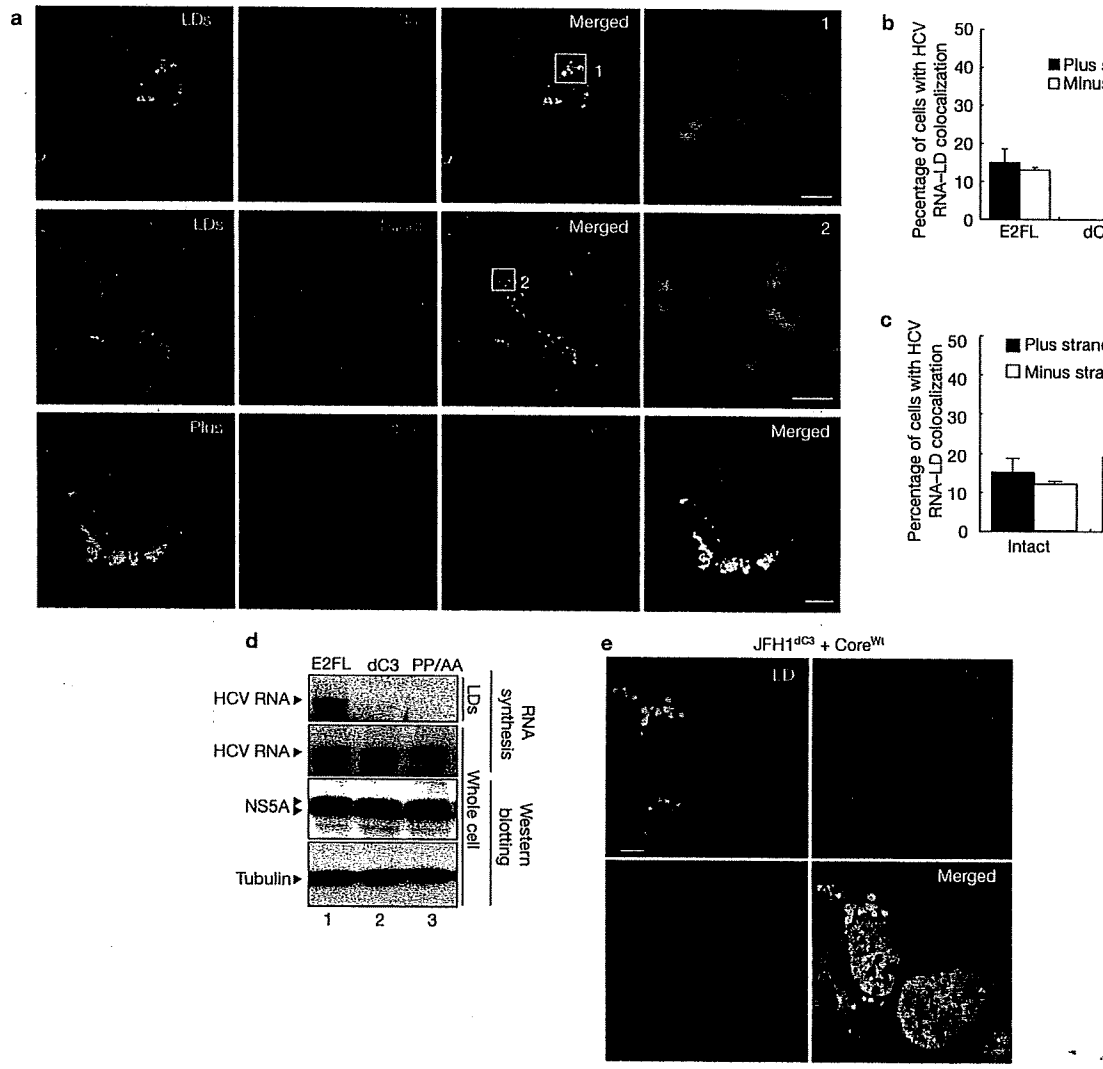

Figure 2 Core-dependent recruitment of active HCV replication complexes to the LD. **(a)** Huh-7 cells transfected with JFH1^{E2FL} RNA were analysed by *in situ* hybridization with strand-specific probes (plus or minus). The cells were labelled to simultaneously visualize lipid droplets (LDs), NS5A and Core (lower panels). Higher-magnification images of area 1 and area 2 are shown in the upper and middle right panels 1 and 2, respectively. Scale bars: 2 μm (panels 1, 2); 10 μm (lower right panel). **(b)** The percentages of JFH1^{E2FL}-, JFH1^{dC3}- and JFH1$^{PP/AA}$-expressing cells positive for overlapping signals for LDs and plus- or minus-strand hepatitis C virus (HCV) RNA ($n > 200$). **(c)** Intact or digitonin and nuclease-treated (dig/nuc) JFH1^{E2FL} replicon-bearing cells were analysed by *in situ* hybridization. The percentages of cells with overlapping signals for LD and plus- or minus-strand HCV RNA are shown ($n > 200$). **(d)** RNA-synthesizing activity in the LD fractions purified from cells transfected with JFH1^{E2FL}, JFH1^{dC3} or JFH1$^{PP/AA}$ RNA (top panel). As a control, HCV RNA synthesis activity in digitonin-permeabilized cells was analysed (second panel from the top). HCV protein levels represented by NS5A are shown, together with the level of tubulin (bottom two panels). **(e)** Localization of plus-strand HCV RNA and Core in JFH1^{dC3} replicon-bearing cells transfected with pcDNA3–Core^{Wt} (Scale bar, 10 μm). Uncropped images of gels are shown in Supplementary Information Fig. S6. All error bars are derived from s.d.

located in the perinuclear region (see Supplementary Information, Fig. S4a). More importantly, in about 20% of these cells, plus- and minus-strand RNAs accumulated around LDs (Fig. 2a, upper and middle panels; 2b) and colocalized with HCV proteins such as Core and NS5A (Fig. 2a, lower panels). No association between HCV RNA and LDs was detected in JFH1^{dC3}- or JFH1$^{PP/AA}$-replicating cells (Fig. 2b). Northern blot analysis revealed that 4.8% and 5.4% of total plus- and minus-strand HCV RNA, respectively, were detected in purified LD fractions of JFH^{E2FL}-replicating cells (data not shown). Induction of LD formation with oleic acid did not affect HCV RNA accumulation around LDs (data not shown). These results provide strong evidence that Core recruits HCV RNA as well as NS proteins to LDs.

The HCV replication complex is compartmentalized by lipid bilayer membranes[16–18]. Therefore, HCV RNA in the complex is resistant to nuclease treatment in digitonin-permeabilized cells[17] (Supplementary Information, Fig. S4b–d). *In situ* hybridization analysis did not reveal a significant difference in the number of cells containing LD-associated HCV RNA before and after nuclease treatment (Fig. 2c), indicating that HCV RNA around LDs is part of the replication complex. An RNA synthesis assay showed that the purified LD fraction from JFH1^{E2FL}-, but not JFH1^{dC3}- or JFH1$^{PP/AA}$-replicating cells, possessed HCV RNA synthesis activity, even though the expression levels of viral proteins and RNA-synthesizing activities in total cell lysates were similar (Fig. 2d). Moreover, the addition of Core^{Wt} rescued the localization of plus- and minus-strand

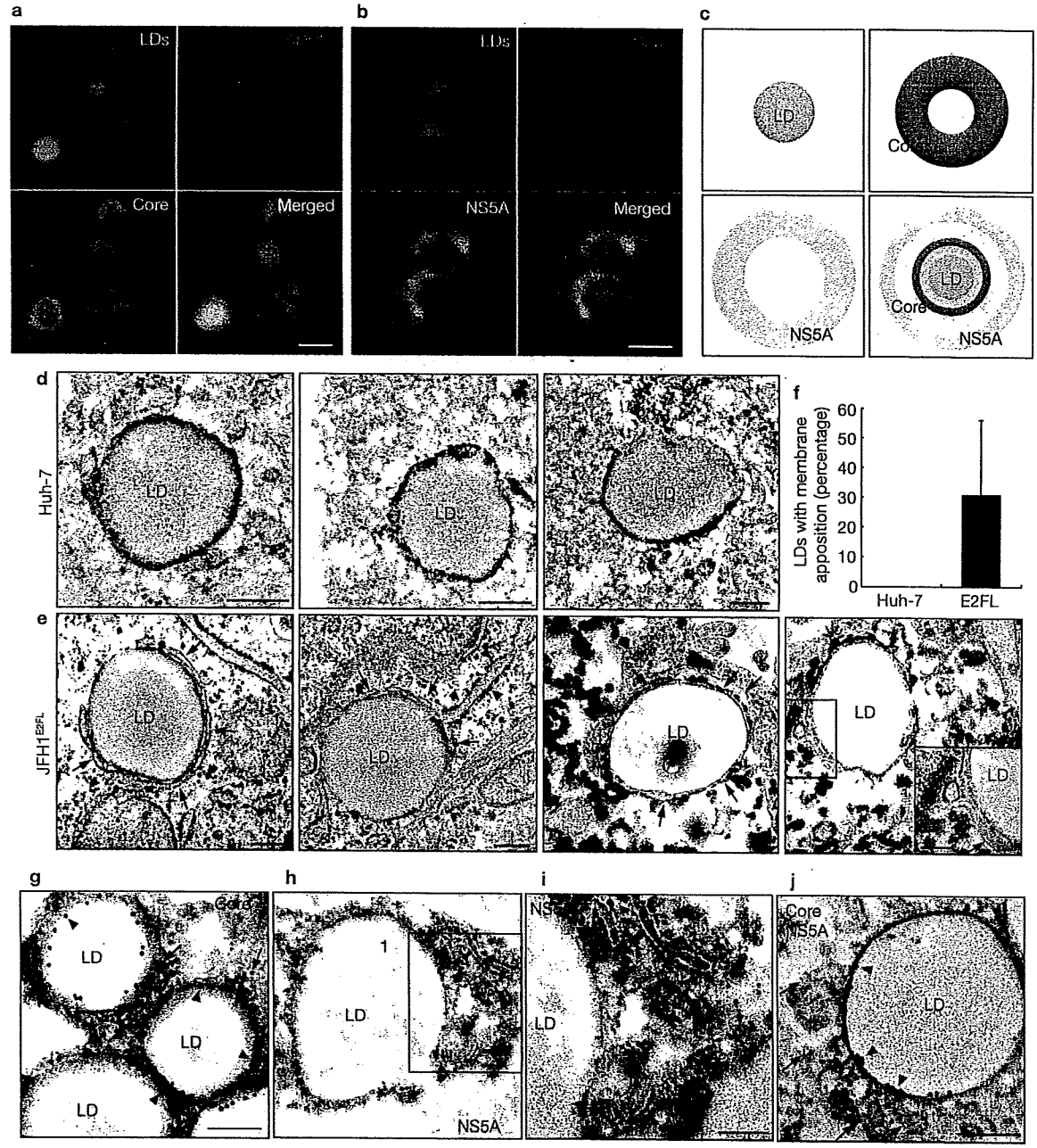

Figure 3 Spatial distribution of Core and NS5A relative to the LD. (**a**, **b**) The localizations of Core, NS5A and ADRP around the lipid droplets (LDs) in JFH1^{E2FL} replicon-bearing cells were analysed using immunofluorescence microscopy. Scale bars, 1 μm. (**c**) Typical images of the localization of LDs, Core, NS5A and merged images are shown with the relative scale of each image. (**d**, **e**) Transmission electron micrographs of LDs in naïve Huh-7 cells and JFH1^{E2FL}-expressing cells. Arrows and arrowheads indicate LD-associated membranes and rough ER membranes, respectively. (**f**) Frequency of LDs with close appositions of membrane cisternae. About 100 Huh-7 cells or JFH1^{E2FL}-expressing cells, respectively, were chosen randomly. LDs with apposed membrane cisternae, as exemplified in panel **e**, were counted as positive. The LDs judged as positive were divided by the total number of LDs. (**g**–**j**) Immunoelectron micrographs of LDs labelled with antibodies against Core (**g**), NS5A (**h**, **i**) or both (**j**) are shown. Panel **i** is a higher magnification of area 1 in panel **h**. In panel **j**, Core and NS5A are labelled with 15 nm and 10 nm gold particles, respectively. Scale bars, 200 nm. All error bars are derived from s.d.

HCV RNA around LDs in JFH^{dC3}-replicating cells (Fig. 2e and data not shown). Both plus- and minus-strand RNA associated with LDs were nuclease resistant (data not shown). These results demonstrate that Core recruits biologically active replication complexes to LDs.

The LD is surrounded by a phospholipid monolayer[19], whereas HCV replication complexes are likely to be surrounded by lipid bilayer membranes[16,17]. Therefore, the replication complexes might not be directly associated with the membranes of LDs. To characterize the colocalization of LDs, viral proteins and replication complexes more precisely, we analysed the localization of NS5A with high-resolution immunofluorescence microscopy. Core was completely colocalized with ADRP, residing on the surface of LDs[20] (Fig. 3a), thus indicating that Core also directly associates with the surface of LDs. More importantly, NS5A mainly localized around the Core-positive area, resulting in a doughnut-shaped signal with a diameter slightly

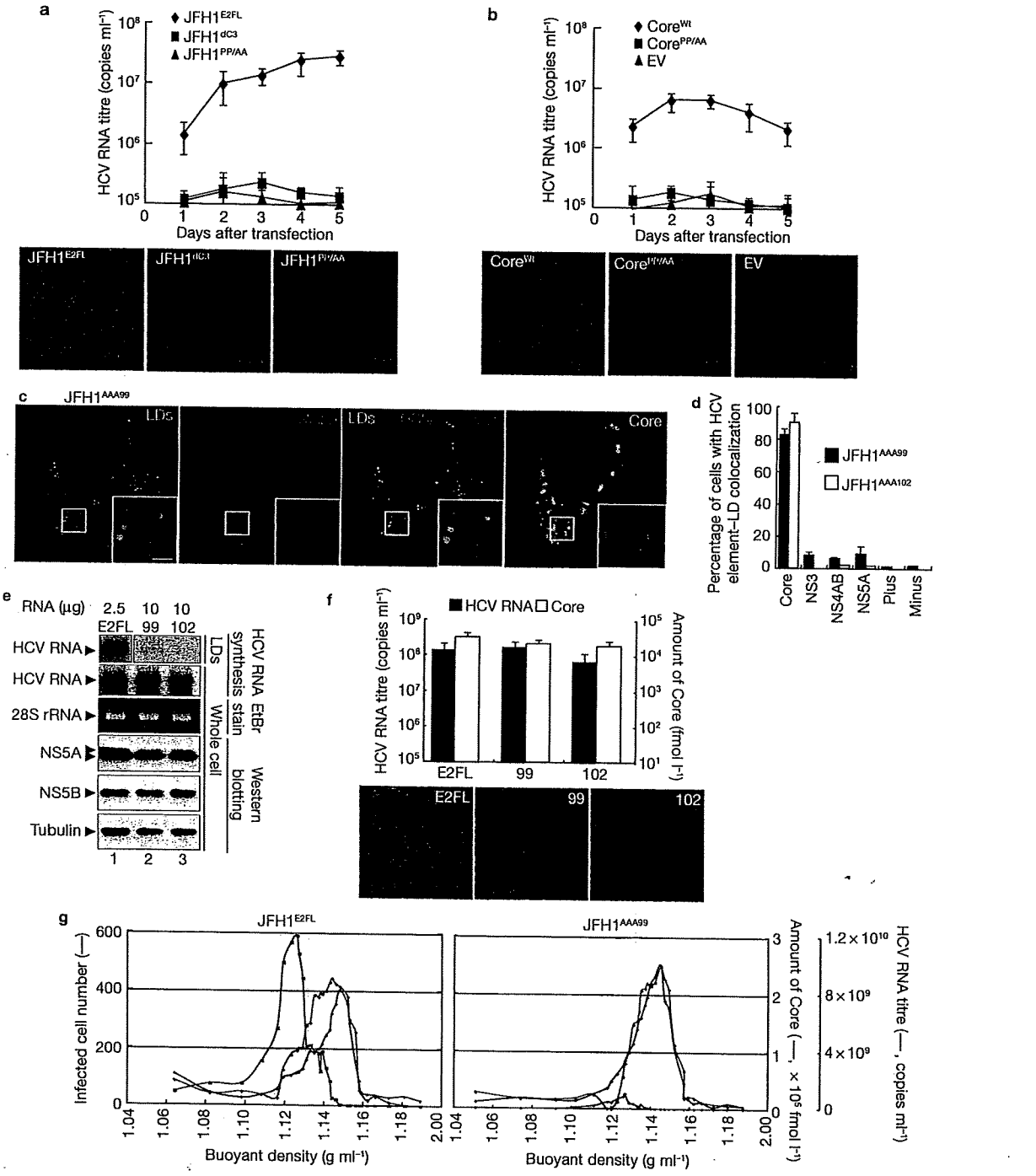

Figure 4 LD associations of Core and NS proteins are necessary for the production of infectious HCV particles. **(a)** The culture medium from JFH1^{E2FL}-, JFH1^{dC3}- or JFH1$^{PP/AA}$-replicating cells was collected at the indicated time points and the titre of hepatitis C virus (HCV) RNA was measured by real-time RT-PCR (upper panel, $n = 3$). The culture medium was added to naïve Huh7.5 cells and, 24 h after inoculation, and cells were labelled with anti-HCV antibodies (lower panels, red). **(b)** JFH1^{dC3} replicon-bearing cells were transfected with pcDNA3 (EV), pcDNA3–Core^{Wt} (Core^{Wt}) or pcDNA3–Core$^{PP/AA}$ (Core$^{PP/AA}$). The level of HCV RNA and the infectivity of the culture medium were examined as described above ($n = 3$). **(c)** Subcellular localization of NS5A and Core in cells expressing JFH1^{AAA99}. The insets are high magnifications of the area of the corresponding panel. Scale bar, 2 μm. **(d)** Percentages of cells in which the signals for given HCV proteins, and plus- and minus-strand HCV RNA, overlapped with those for LDs ($n > 200$). **(e)** Different amounts of JFH1^{E2FL} (E2FL), JFH1^{AAA99} (99) or JFH1^{AAA102} (102) RNAs, respectively, were transfected into the same number of Huh-7 cells. HCV RNA synthesis activity in purified LD fractions (LD) and whole-cell lysates (whole cell) was analysed (HCV RNA synthesis). 28S rRNA was used as a control. Western blot analysis of NS5A, NS5B and tubulin in cells is also shown. All the RNA samples in the top panel were run on the same gel. **(f)** Analysis of HCV released from cells expressing JFH1^{E2FL}, JFH1^{AAA99} or JFH1^{AAA102}. HCV RNA titres (black bars) and amounts of Core (white bars) accumulated in the culture medium at 5 d after RNA transfection were measured (upper panel, $n = 3$). Infectivity of the culture medium for naïve Huh-7.5 cells was analysed as described above (lower panels). **(g)** Concentrated culture medium from JFH1^{E2FL}- and JFH1^{AAA99}-replicating cells was fractionated using 20–50% sucrose density-gradient centrifugation at 100,000 *g* for 16 h. For each fraction, the amounts of Core (black line), HCV RNA (blue line) and infectivity (represented by infected cell numbers in a well; red line) are plotted against the buoyant density (*x*-axis) ($n = 3$). Uncropped images of gels are shown in Supplementary Information Fig. S6. All error bars are derived from s.d.

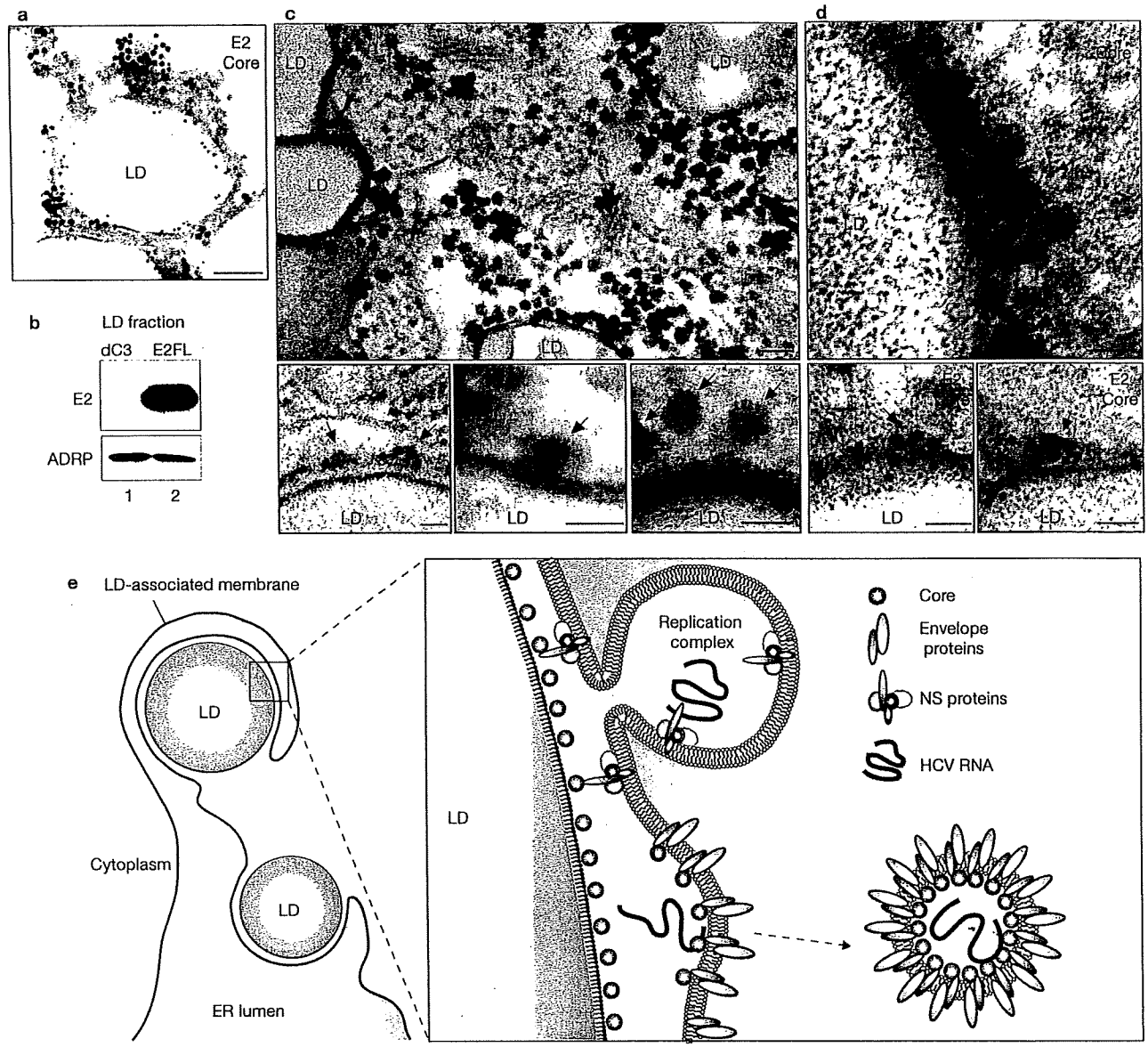

Figure 5 Virus-assembly takes place around the LDs. **(a)** Immunoelectron microscopic detection of E2 and Core in JFH1^{E2FL}-replicating cells. E2 and Core are labelled with 15 nm and 10 nm gold particles, respectively. **(b)** Western blot analysis of the lipid droplet (LD) fraction from JFH1^{E2FL} and JFH1^{dC3} replicon-bearing cells with anti-E2 and anti-ADRP antibodies. **(c)** Transmission electron micrographs of JFH1^{E2FL}-replicating cells. Arrows indicate virus-like particles. **(d)** Immunoelectron micrographs of LDs labelled with antibodies against Core (10 nm) and E2 (15 nm) are shown. Arrows show Core in electron-dense granules. Scale bar: **a** and upper panel of **c**: 100 nm; in **d** and lower panels of **c**: 50 nm. **(e)** A model for the production of infectious hepatitis C virus (HCV). Core mainly localizes on the monolayer membrane that surrounds the LD. HCV induces the apposition of the LD to the endoplasmic reticulum (ER)-derived bilayer membranes (LD-associated membrane). Core recruits NS proteins, as well as replication complexes, to the LD-associated membrane. NS proteins around the LD can then participate in infectious virus production. E2 also localizes around the LD. Through these associations, virion assembly proceeds in this local environment. Uncropped images of gels are shown in Supplementary Information Fig. S6.

larger than that of Core (Fig. 3b). The LD-proximal NS5A signal partially overlapped with the Core signal (Fig. 3b, c, grey). This concentric staining pattern was also observed with the other NS proteins (Supplementary Information, Fig. S5a), indicating that NS proteins associate with Core on the surface of LDs. Electron microscopic analysis only rarely revealed a close association of LDs with other organelles in naïve Huh-7 cells (Fig. 3d, f). However, in the case of JFH1^{E2FL}-replicating cells, about 30% of the LDs were in close proximity to membrane cisternae (Fig. 3e, arrows; 3f), arguing for a HCV-induced membrane rearrangement around LDs. Core was mainly located on the periphery of LDs, and occasionally signals were observed in more distal areas of the LDs (Fig. 3g, arrowheads and arrows, respectively). Although some NS5A signals were observed on the surface of the LD, the majority of NS5A signals were detected more distal of LDs (Fig. 3h, i). Furthermore, we often observed membrane cisternae as white lines in the same area as NS5A signals (Fig. 3i, arrows). When the same section was labelled with anti-Core and anti-NS5A antibodies, Core was detected on the surface of the LDs, whereas NS5A was mainly observed in the peripheral area of the LDs (Fig. 3j, arrowheads and arrows, respectively). In summary, these results show that Core recruits NS proteins, as well as HCV replication complexes, to the LD-associated membranes.

The above results prompted us to ask whether Core–LD colocalization is important for the production of infectious virus particles. JFH1^{E2FL}-replicating cells released virions into the culture medium and these viruses were highly infectious for naïve Huh-7.5 cells[11,21], although culture medium from JFH1$^{PP/AA}$- or JFH1^{dC3}-replicating cells did not contain significant levels of HCV RNA and infectious virus (Fig. 4a). However, following trans-complementation with Core^{Wt}, a high titre of HCV RNA and infectious virus could be rescued from JFH1^{dC3}-replicating cells (Fig. 4b; and see Supplementary Information, Fig. S5b, c). In contrast, the production of infectious viruses was not rescued by trans-complementation with Core$^{PP/AA}$ (Fig. 4b). RNA-binding properties and oligomerization of Core^{Wt} and Core$^{PP/AA}$, which are both necessary for virus assembly, were similar (Supplementary Information, Fig. S5d; ref. 22), arguing that the primary defect of this mutant in preventing infectious virus production is the inability to associate with LDs.

To investigate the contribution of NS proteins around LDs to infectious virus production, we used variants of NS5A, which were not recruited to LDs even in the presence of Core. We assumed that NS5A was crucial for recruiting other NS proteins to LDs, because the level of NS5A recruited to LDs via Core was higher than the levels of the other recruited NS proteins (Fig. 1c, JFH1^{E2FL}). Using alanine-scanning mutagenesis within the NS5A coding region of JFH1^{E2FL}, we generated two mutants, JFH1^{AAA99} and JFH1^{AAA102}, in which the amino-acid sequence APK (aa 99–101 of NS5A) or PPT (aa 102–104 of NS5A) was replaced by AAA (Supplementary Information, Fig. S1). In JFH1^{AAA99}- and JFH1^{AAA102}-replicating cells, NS5A was rarely detected around LDs, whereas Core was still localized to LDs (Fig. 4c, d). Importantly, these mutations impaired not only the NS5A association with LDs, but also the recruitment of other NS proteins and viral RNAs to LDs (Fig. 4d). These results indicate that NS5A is a key protein that recruits replication complexes to LDs. Importantly, HCV RNA synthesis activity in the LD fractions from these mutant JFH1-replicating cells was also severely impaired (Fig. 4e), corroborating the lack of association of HCV replication complexes with LDs.

To investigate the infectious virus production of these NS5A mutants, we prepared cells expressing similar levels of HCV proteins and RNA by adjusting the amount of transfected HCV RNA (Fig. 4e). This was necessary, because replication activities of these mutants were lower compared with JFH1^{E2FL}. Under these conditions, the amounts of Core and HCV RNA that were released into the culture medium from cells transfected with the mutants were comparable to JFH^{E2FL} (Fig. 4f, upper graph). However, infectivity titres of the mutants were severely reduced (Fig. 4f, lower panels). In sucrose density-gradient centrifugation of culture medium from JFH1^{E2FL}-bearing cells, two types of HCV particles were detected: low-density particles (about 1.12 g ml^{-1}) with high infectivity (Fig. 4g, green area of JFH1^{E2FL}), and high-density particles (about 1.15 g ml^{-1}) without infectivity (yellow area). This result indicates that only a minor portion of released HCV particles is infectious, whereas the majority of released particles lack infectivity. In contrast, cells bearing the JFH1^{AAA99} mutant almost exclusively released non-infectious particles of around 1.15 g ml^{-1}, whereas infectious particles were barely detectable (Fig. 4g, JFH1^{AAA99}). Taken together, these results provide convincing evidence that the association of NS proteins and replication complexes around LDs is critical for producing infectious viruses, whereas production of non-infectious viruses seems to follow a different pathway.

The results described so far imply that some step(s) of HCV assembly take place around LDs. To explore this possibility, we analysed the distribution of the major envelope protein E2 around the LD. Electron microscopic analysis revealed that, in about 90% of JFH1^{E2FL}-replicating cells, E2 was localized in the peripheral area of the LDs (Fig. 5a, large grains). This labelling pattern was similar to the one observed for NS5A (Fig. 3j), indicating that E2 also localizes on the LD-associated membranes. Western blot analysis of the LD fraction supported this conclusion, because the LD fraction that was purified from JFH1^{E2FL}-replicating cells, but not from JFH1^{dC3}-replicating cells, contained E2 (Fig. 5b). Furthermore, spherical virus-like particles with an average diameter of about 50 nm were observed around LDs in JFH1^{E2FL}-replicating cells (Fig. 5c, upper panel). These particles were never observed in naïve Huh-7 cells. A more refined analysis indicates that these particles are closely associated with membranes in close proximity to LDs (Fig. 5c, lower panels, arrows). Finally, these particles around the LDs reacted with Core- and E2-specific antibodies, arguing that the particles represent true HCV virions (Fig. 5d). These results suggest that infectious HCV particles are generated from the LD-associated membranous environment.

In this study, we have demonstrated that Core recruits NS proteins, HCV RNAs and the replication complex to LD-associated membranes. Mutations of Core and NS5A (Fig. 4), which failed to associate with LDs, impaired the production of infectious virus. We note that the mutant Core retains the ability to interact with RNA (Supplementary Information, Fig. S5b) and to assemble into nucleocapside[22]. Similarly, the NS5A mutant still supports viral genome replication and the formation of capsids or virus-like particles, arguing that the introduced mutations in Core and NS5A do not affect overall protein folding, stability or function (Fig. 4). Taken together, the data show that the association of HCV proteins with LDs is important for the production of infectious viral particles (Fig. 5e).

Our results also indicate that NS proteins around the LDs participate in the assembly of infectious virus particles. In one scenario, NS proteins may indirectly contribute to the different steps of virus production — for example, by establishing the microenvironment around the LDs that is required for infectious virus production. Alternatively, NS proteins around the LDs may directly participate in virus production — for example, as components of the replication complex that provide the RNA genome to the assembling nucleocapsid.

In support of the role of LDs in virus formation, we observed that colocalization of HCV protein with LDs was low in cases of the chimera Jc1, supporting up to 1,000-fold higher infectivity titres compared with JFH1 (ref. 13). In a Jc1-infected cell, only about 20% of LDs demonstrated detectable colocalization with Core, but this value increased to 80% in the case of a Jc1 mutant lacking most of the envelope glycoprotein genes and thus being unable to produce infectious virus particles (data not shown). This inverse correlation between the efficiency of virus production and Core protein accumulation on LDs indicates that rapid assembly and virus release results in the rapid liberation of HCV proteins from the LDs.

Steatosis and abnormal lipid metabolism caused by chronic HCV infection may be linked to enhanced LD formation[14]. In fact, the overproduction of LDs is induced by Core (Supplementary Information, Fig. S3) and HCV also induces membrane rearrangements around LDs (Fig. 3d–f). Our findings suggest that excessive Core-dependent formation of LDs

and membrane rearrangements are required to supply the necessary microenvironment for virus production. NS proteins and HCV RNA seem to be translocated from the ER to the LD-associated membranes. Interestingly, the LD-associated membranes were occasionally found in continuity with ribosome-studded rough ER (Fig. 3e, arrowheads). Thus, at least parts of the LD-associated membranes are likely to be derived from ER membranes. ER marker proteins, however, were not detected in the LD fraction, suggesting that the LD-associated membrane is characteristically distinct from that of ER membranes.

To our knowledge, this is the first report showing that LDs are required for the formation of infectious virus particles. The fact that capsid protein of the hepatitis G virus also localizes to LDs[15] indicates that LDs might be important for the production of other viruses as well. Our findings demonstrate a novel function of LDs, provide an important step towards elucidating the mechanism of HCV virion production and open new avenues for novel antiviral intervention. □

METHODS

Antibodies. The antibodies used for immunoblotting and immunolabelling were specific for Core (#32-1 and RR8); E2 (AP-33 (ref. 23); 3/11, CBH5 and Flag M2 (Sigma-Aldrich, St Louis, MO); NS3 (R212)[17]; NS4A and 4B (PR12); NS5A (NS5ACL1); NS5B (NS5B-6 and JFH1-1)[24]; ADRP (Progen Biotechnik, Heidelberg, Germany); tubulin (Oncogene Research Products, MA, USA); Grp78 (StressGen, Victoria, Canada); PDI (StressGen); and Calnexin-NT (StressGen). Antibodies specific for Core (#32-1 and RR8), NS3 (R212) and NS4AB (PR12) were gifts from Dr Kohara (The Tokyo Metropolitan Institute of Medical Science, Japan). Anti-E2 antibody (AP-33) was provided by Dr Patel (MRC Virology Unit, UK). Anti-NS5B (NS5B-6) antibody was kindly provided by Dr Fukuya (Osaka University, Japan). Rabbit polyclonal antibodies specific for NS5A were raised against a bacterially expressed GST-NS5A (1–406 aa) fusion protein. In the case of the HCV chimeras Con1/C3 and H77/C3, immunofluorescence analyses were performed by using the following antibodies: Core (C7/50)[5], a JFH1 NS3-specific rabbit polyclonal antiserum; NS4B (#86)[25]; and NS5A (Austral Biologicals, San Ramon, CA).

Indirect immunofluorescence analysis. Indirect immunofluorescence analysis was performed essentially as described previously[17], with slight modifications. Cells transfected with JFH1 RNA were seeded onto a collagen-coated Labtech II 8-well chamber (Nunc, NY, USA). The coating with collagen was performed using rat-tail collagen type I (BD Bioscience, Palo Alto, CA) according to manufacturer's instructions. Three days after seeding, the cells were washed twice with phosphate-buffered saline (PBS; 137 mM NaCl, 2.7 mM KCl, 4.3 mM Na_2HPO_4 and 1.4 mM KH_2PO_4) and fixed with fixation solution (4% paraformaldehyde and 0.15 M sodium cacodylate at pH 7.4) for 15 min at room temperature. After washing with PBS, the cells were permeabilized with 0.05% Triton X-100 in PBS for 15 min at room temperature. For the precise localization of the proteins, the cells were permeabilized with 50 μg ml^{-1} of digitonin in PBS for 5 min at room temperature[26]. After incubating the cells with blocking solution (10% fetal bovine serum and 5% bovine serum albumin (BSA) in PBS) for 30 min, the cells were incubated with the primary antibodies. The fluorescent secondary antibodies were Alexa 568- or Alexa 647-conjugated anti-mouse or anti-rabbit IgG antibodies (Invitrogen, Carlsbad, CA). Nuclei were labelled with 4',6-diamidino-2-phenylindole (DAPI). LDs were visualized with BODIPY 493/503 (Invitrogen). Analyses of JFH1 were performed on a Leica SP2 confocal microscope (Leica, Heidelberg, Germany). Analysis of the Con1/C3 and the H77/C3 chimeras was performed in the same way, except that imaging was performed on a Nikon C1 confocal microscope (Nikon, Tokyo, Japan).

Electron microscopy. For conventional electron microscopy, cells cultured in plastic Petri dishes were processed *in situ*. The cells were fixed in 2.5% glutaraldehyde and 0.1 M sodium phosphate (pH 7.4), and then in OsO_4 and 0.1 M sodium phosphate (pH 7.4). The cells were then dehydrated in a graded ethanol series and embedded in an epoxy resin. Ultrathin sections were cut perpendicular to the base of the dish. For immuno-electron microscopy, cells were detached from the dish with a cell scraper after fixation in 4% paraformaldehyde, 0.1% glutaraldehyde and 0.1 M sodium phosphate (pH 7.4) for 24 h, and washed in 0.1 M lysine, 0.1 M sodium phosphate (pH 7.4) and 0.15 M sodium chloride. After dehydrating the cells in a graded series of cold ethanol, they were embedded in Lowicryl K4M at −20 °C. Ultrathin sections were labelled with primary antibodies and colloidal gold particles (15 nm) conjugated to anti-mouse IgG or anti-rabbit IgG antibodies. For double labelling, colloidal gold particles with different diameters (10 nm and 15 nm) conjugated to anti-mouse IgG or anti-rabbit antibodies were used. Samples were observed after staining with uranyl acetate and lead citrate with a JEM 1010 electron microscope at the accelerating voltage of 80 kV. Anti-Core (#32-1 and RR88), anti-NS5A (NS5ACL1) and anti-E2 (Flag M2) antibodies were used.

Preparation of the lipid droplets. Cells at a confluency of ~80% on a dish with a diameter of 14 cm were scraped in PBS. The cells were pelleted by centrifugation at 1,500 rpm. The pellet was resuspended in 500 μl of hypotonic buffer (50 mM HEPES, 1 mM EDTA and 2 mM $MgCl_2$ at pH 7.4) supplemented with protease inhibitors (Roche Diagnostics, Basel, Switzerland) and was incubated for 10 min at 4 °C. The suspension was homogenized with 30 strokes of a glass Dounce homogenizer using a tight-fitting pestle. Then, 50 μl of 10× sucrose buffer (0.2 M HEPES, 1.2 M KoAc, 40 mM $Mg(oAc)_2$ and 50 mM DTT at pH 7.4) was added to the homogenate. The nuclei were removed by centrifugation at 2,000 rpm for 10 min at 4 °C. The supernatant was collected and centrifuged at 16,000 *g* for 10 min at 4 °C. The supernatant (S16) was mixed with an equal volume of 1.04 M sucrose in isotonic buffer (50 mM HEPES, 100 mM KCl, 2 mM $MgCl_2$ and protease inhibitors). The solution was set at the bottom of 2.2-ml ultracentrifuge tube (Hitachi Koki, Tokyo, Japan). One milliliter of isotonic buffer was loaded onto the sucrose mixture. The tube was centrifuged at 100,000 *g* in an S55S rotor (Hitachi Koki) for 30 min at 4 °C. After the centrifugation, the LD fraction on the top of the gradient solution was recovered in isotonic buffer. The suspension was mixed with 1.04 M sucrose and centrifuged again at 100,000 *g*, as described above, to eliminate possible contamination with other organelles. The collected LD fraction was used for western blotting or the HCV RNA synthesis assay.

HCV RNA synthesis assay. An assay of HCV RNA synthesis using digitonin-permeabilized cells was performed as described previously[17]. For RNA synthesis assays using the LD fraction, the LD fraction collected by sucrose-gradient sedimentation was suspended in buffer B, which contained 2 mM manganese (II) chloride, 1 mg ml^{-1} acetylated BSA (Nacalai Tesque, Kyoto, Japan), 5 mM phosphocreatine (Sigma), 20 units/ml creatine phosphokinase (Sigma), 50 μg ml^{-1} actinomycin D, 500 μM ATP, 500 μM CTP, 500 μM GTP (Roche Diagnostics) and 1.85 MBq of [α-^{32}P] UTP (GE Healthcare, Little Chalfont, UK), and incubated at 27 °C for 4 h. The reaction products were analysed by gel electrophoresis followed by autoradiography.

Note: Supplementary Information is available on the Nature Cell Biology website.

ACKNOWLEDGEMENTS

We thank T. Fujimoto and Y. Ohsaki at Nagoya University for helpful discussions and technical assistance. Y.M. is a recipient of a JSPS fellowship. K.S. is supported by Grants-in-Aid for cancer research and for the second-term comprehensive 10-year strategy for cancer control from the Ministry of Health, Labour and Welfare, as well as by a Grant-in-Aid for Scientific Research on Priority Areas "Integrative Research Toward the Conquest of Cancer" from the Ministry of Education, Culture, Sports, Science and Technology of Japan. T.W. is also supported, in part, by a Grant-in-Aid for Scientific Research from the Japan Society for the Promotion of Science; and by the Research on Health Sciences Focusing on Drug Innovation from the Japan Health Sciences Foundation. R.B. is supported by the Sonderforschungsbereich 638 (Teilprojekt A5) and the Deutsche Forschungsgemeinschaft (BA1505/2-1). M.Z. and R.B. thank the Nikon Imaging Center at the University of Heidelberg for providing access to their confocal fluorescence microscopes and Ulrike Engel for the excellent support.

AUTHOR CONTRIBUTIONS

Y.M. and K.S. planned experiments and analyses. Y.M. was responsible for experiments for Figs 1, 2, 3a–c, 4a–e and 5b. K.A., N.U., electron microscopy; T.H., Fig. 1e; M.Z., R.B., Fig. S2e; and K.S. and K.W., Fig. 4f–g. T.W. provided JFH1 strain. Y.M. and K.S. wrote the manuscript. All authors discussed the results and commented on the manuscript.

COMPETING FINANCIAL INTERESTS
The authors declare no competing financial interests.

Published online at http://www.nature.com/naturecellbiology/
Reprints and permissions information is available online at http://npg.nature.com/reprintsandpermissions/

1. Martin, S. & Parton, R. G. Lipid droplets: a unified view of a dynamic organelle. *Nature Rev. Mol. Cell Biol.* **7**, 373–378 (2006).
2. Blanchette-Mackie, E. J. *et al.* Perilipin is located on the surface layer of intracellular lipid droplets in adipocytes. *J. Lipid Res.* **36**, 1211–1226 (1995).
3. Vock, R. *et al.* Design of the oxygen and substrate pathways. VI. structural basis of intracellular substrate supply to mitochondria in muscle cells. *J. Exp. Biol.* **199**, 1689–1697 (1996).
4. Liang, T. J. *et al.* Viral pathogenesis of hepatocellular carcinoma in the United States. *Hepatology* **18**, 1326–1333 (1993).
5. Moradpour, D., Englert, C., Wakita, T. & Wands, J. R. Characterization of cell lines allowing tightly regulated expression of hepatitis C virus core protein. *Virology* **222**, 51–63 (1996).
6. Deleersnyder, V. *et al.* Formation of native hepatitis C virus glycoprotein complexes. *J. Virol.* **71**, 697–704 (1997).
7. Kato, N. *et al.* Molecular cloning of the human hepatitis C virus genome from Japanese patients with non-A, non-B hepatitis. *Proc. Natl Acad. Sci. USA* **87**, 9524–9528 (1990).
8. Hijikata, M. & Shimotohno, K. [Mechanisms of hepatitis C viral polyprotein processing]. *Uirusu* **43**, 293–298 (1993).
9. Dubuisson, J., Penin, F. & Moradpour, D. Interaction of hepatitis C virus proteins with host cell membranes and lipids. *Trends Cell Biol.* **12**, 517–523 (2002).
10. Wakita, T. *et al.* Production of infectious hepatitis C virus in tissue culture from a cloned viral genome. *Nature Med.* **11**, 791–796 (2005).
11. Lindenbach, B. D. *et al.* Complete replication of hepatitis C virus in cell culture. *Science* **309**, 623–626 (2005).
12. Zhong, J. *et al.* Robust hepatitis C virus infection in vitro. *Proc. Natl Acad. Sci. USA* **102**, 9294–9299 (2005).
13. Pietschmann, T. *et al.* Construction and characterization of infectious intragenotypic and intergenotypic hepatitis C virus chimeras. *Proc. Natl Acad. Sci. USA* **103**, 7408–7413 (2006).
14. Moriya, K. *et al.* Hepatitis C virus core protein induces hepatic steatosis in transgenic mice. *J. Gen. Virol.* **78**, 1527–1531 (1997).
15. Hope, R. G., Murphy, D. J. & McLauchlan, J. The domains required to direct core proteins of hepatitis C virus and GB virus-B to lipid droplets share common features with plant oleosin proteins. *J. Biol. Chem.* **277**, 4261–4270 (2002).
16. Egger, D. *et al.* Expression of hepatitis C virus proteins induces distinct membrane alterations including a candidate viral replication complex. *J. Virol.* **76**, 5974–5984 (2002).
17. Miyanari, Y. *et al.* Hepatitis C virus non-structural proteins in the probable membranous compartment function in viral genome replication. *J. Biol. Chem.* **278**, 50301–50308 (2003).
18. Quinkert, D., Bartenschlager, R. & Lohmann, V. Quantitative analysis of the hepatitis C virus replication complex. *J. Virol.* **79**, 13594–13605 (2005).
19. Tauchi-Sato, K., Ozeki, S., Houjou, T., Taguchi, R. & Fujimoto, T. The surface of lipid droplets is a phospholipid monolayer with a unique fatty acid composition. *J. Biol. Chem.* **277**, 44507–44512 (2002).
20. Londos, C., Brasaemle, D. L., Schultz, C. J., Segrest, J. P. & Kimmel, A. R. Perilipins, ADRP, and other proteins that associate with intracellular neutral lipid droplets in animal cells. *Semin. Cell Dev. Biol.* **10**, 51–58 (1999).
21. Blight, K. J., McKeating, J. A. & Rice, C. M. Highly permissive cell lines for subgenomic and genomic hepatitis C virus RNA replication. *J. Virol.* **76**, 13001–13014 (2002).
22. Klein, K. C., Dellos, S. R. & Lingappa, J. R. Identification of residues in the hepatitis C virus core protein that are critical for capsid assembly in a cell-free system. *J. Virol.* **79**, 6814–6826 (2005).
23. Owsianka, A. *et al.* Monoclonal antibody AP33 defines a broadly neutralizing epitope on the hepatitis C virus E2 envelope glycoprotein. *J Virol* **79**, 11095–11104 (2005).
24. Ishii, N. *et al.* Diverse effects of cyclosporine on hepatitis C virus strain replication. *J. Virol.* **80**, 4510–4520 (2006).
25. Lohmann, V., Korner, F., Herian, U. & Bartenschlager, R. Biochemical properties of hepatitis C virus NS5B RNA-dependent RNA polymerase and identification of amino acid sequence motifs essential for enzymatic activity. *J Virol* **71**, 8416–8428 (1997).
26. Ohsaki, Y., Maeda, T. & Fujimoto, T. Fixation and permeabilization protocol is critical for the immunolabeling of lipid droplet proteins. *Histochem. Cell Biol.* **124**, 445–452 (2005).